LA-UR-16-28000
Approved for public release; distribution is unlimited.

Title: Literature Review: Weldability of Iridium DOP-26 Alloy for General Purpose Heat Source

Author(s): Burgardt, Paul
Pierce, Stanley W.

Intended for: Report

Issued: 2016-10-19

LITERATURE REVIEW:

WELDABILITY OF IRIDIUM DOP-26 ALLOY

FOR

GENERAL PURPOSE HEAT SOURCE

P. Burgardt, Sigma

S. W. Pierce, MET-1

Los Alamos National Laboratory

Los Alamos, NM

August 24, 2016

INTRODUCTION

The basic purpose of this paper is to provide a literature review relative to fabrication of the General Purpose Heat Source (GPHS) that is used to provide electrical power for deep space missions of NASA. The particular fabrication operation to be addressed here is arc welding of the GPHS encapsulation. A considerable effort was made to optimize the fabrication of the fuel pellets and of other elements of the encapsulation; that work will not be directly addressed in this paper.

This report consists of three basic sections: 1) a brief description of the GPHS will be provided as background information for the reader; 2) mechanical properties and the optimization thereof as relevant to welding will be discussed; 3) a review of the arc welding process development and optimization will be presented. Since the welding equipment must be upgraded for future production, some discussion of the historical establishment of relevant welding variables and possible changes thereto will also be discussed.

BASIC DESCRIPTION OF THE GPHS

For deep space NASA missions, electric power generation is problematic once the probe is far enough from the sun that normal photocell arrays will provide insufficient power. Therefore, on those missions a radioisotope thermoelectric power generator (RTG) is used. The essential concept behind a RTG is to convert the heat from radioactive decay into useful electrical power. An interesting side benefit of this power generation method is that there is considerable excess heat available that can be used to warm certain temperature sensitive instruments that would otherwise become too cold during these missions (although this generally accomplished by additional smaller encapsulations specifically designed for this purpose).

The radioactive isotope used in the GPHS is Pu^{238}. This isotope of plutonium has a half-life of 87.4 years and generates about 0.5 watts of heat per gram of material primarily through alpha decay. In order to stabilize the plutonium metal as well as possible, the metal is converted into oxide and made into pellets that fit inside the cladding envelope. The GPHS fueled clad contains about 150 grams of $Pu^{238}O_2$ pressed into a single pellet. Each GPHS units generates about 60 watts of heat, which is converted into about 4.5 watts of electrical power by thermoelectric generator modules. Reportedly, the fueled clads when inside the thermoelectric generator modules are operating at a temperature of about 1250 C. A picture of the GPHS is shown in Figure 1. As can be seen, the GPHS clad consists of two symmetric formed cups that are welded at the middle. A frit is installed on one end of the clad to allow the accumulating helium to escape.

This report is primarily concerned with welding of the GPHS cladding material. Therefore, some discussion of that material choice is warranted. There are two basic design considerations for the cladding material that are of critical importance to the program. First, the cladding material must have the best possible corrosion resistance. Once the GPHS units are delivered for assembly and awaiting launch, they will reside in an atmospheric environment (probably with relatively high humidity) for a considerable time at a high temperature. Therefore, the cladding material must not degrade appreciably in that environment. The second critical design

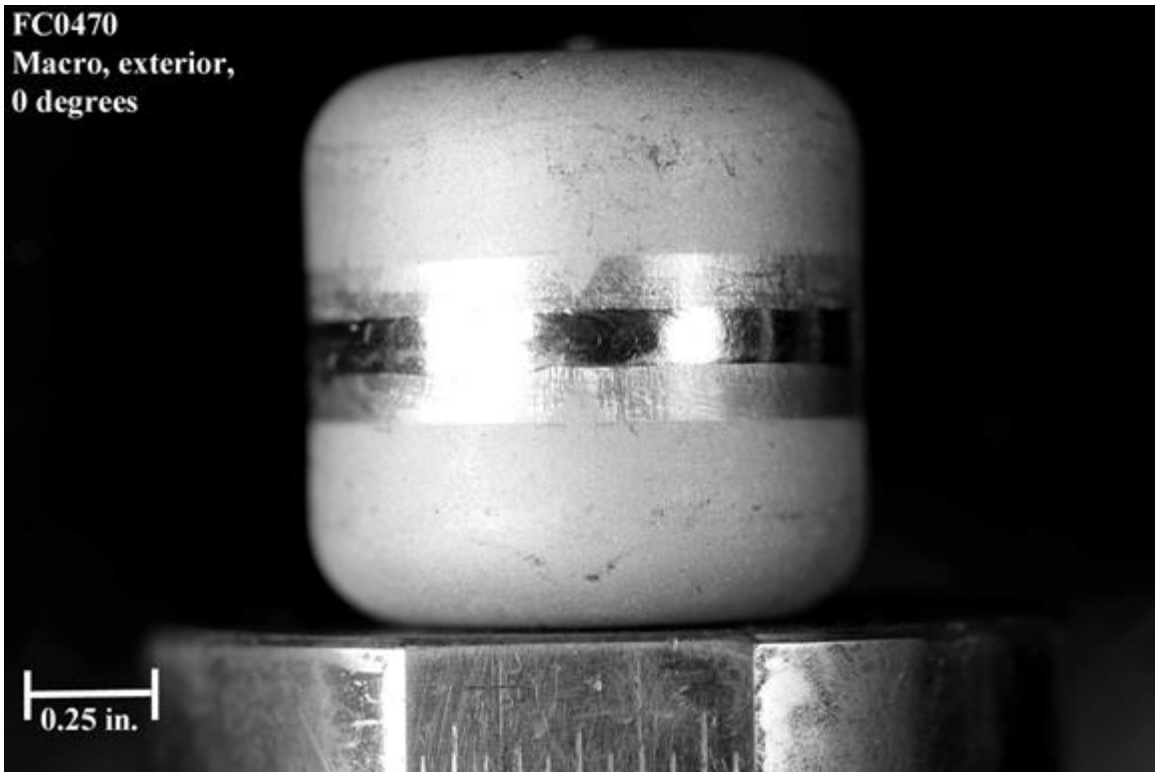

Figure 1: Picture of a GPHS showing the shape and dimensions of the unit.

requirement is that the cladding material must have the best possible chance of staying intact during a launch failure in order to prevent environmental contamination by the highly radioactive fuel material. This basically means that the cladding material must have good ductility at an elevated temperature and in a high strain rate event. In response to this requirement, the cladding material is designed to have optimal ductility at 980 C and in an event corresponding to being struck by a blunt object traveling at a speed of about 61 m/s (200 fps). The primary concern for welding is to produce an optimized high strain rate ductility in the weld metal.

BASE METAL CONSIDERATIONS

The following brief discussion of the base metal is a paraphrasing of language in a report by: T.G. George and M.F. Stevens [1]. The need for good high temperature properties clearly dictates that some refractory be chosen as the cladding material. In order to provide heat source containment in a possible accident, the chosen cladding material must have good oxidation resistance. Additionally, the GPHS when in the RTG spends considerable time at elevated temperature in contact with graphite, where some carbon diffusion into the clad is possible. Therefore, the clad material must form no low melting point eutectics with carbon. Unfortunately, the more common refractories, such as Ta for example, undergo substantial oxidation at elevated temperature. Therefore, the somewhat exotic metal Iridium was chosen as the base element for the cladding because: it is considered to be the most corrosion resistant of all the elements, it has the highest melting point of any fcc metal (2443 C) and the second highest shear modulus (220 GN/m2 at RT) of the elements and forms no low temperature carbon eutectic. Its drawback in this application is that the ductility of pure iridium

is significantly reduced for T < 700 C. The brittle behavior is presumably due to the peculiar directionality of its atomic binding forces along its principal symmetry axes. This results in its mechanical behavior being more similar to a bcc or hcp metal. The pure metal also tends to be considerably notch sensitive and its ductility does seem to be significantly strain rate dependent.

As is true of most pure metals, it is difficult to achieve useful structural properties of the material without some alloying additions because of the resulting coarse grain structure that would be found in any casting (and in welding). Therefore, a grain refining addition is usually used. In this case, a tungsten addition of 0.3 w/o (weight %) is used and seems about optimal in this regard. Thus, the baseline cladding material for the GPHS is: Ir + 0.3W. Unfortunately, the Ir + 0.3W alloy has quite limited impact ductility, especially at low temperatures. Therefore, considerable research was undertaken to search for other alloying additions that would improve the high strain rate ductility. This led to a series of alloys known as the DOP materials (DOP stands for dopant and DOP is apparently pronounced “dope”). It was found that minor additions of Th, Al, Fe, Ni and Rh substantially improved impact ductility apparently by improving grain boundary cohesion. It appears that a combined content of these elements should be about 200 at-ppm. In this regard, thorium additions were found to be most beneficial. Figure 2 shows data for Th additions illustrating that about 200 ppm by weight addition of Th produces optimal impact ductility. The figure is from: C.T. Liu, H. Inouye and A.C. Schaffhouser [2].

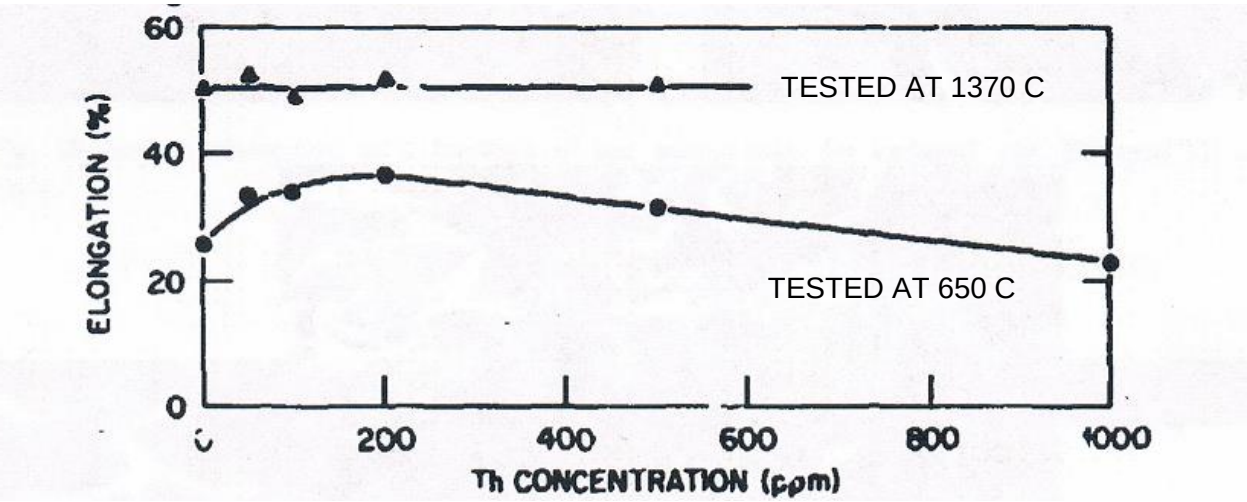

Figure 2: Mechanical test data for Ir + 0.3 W doped with thorium (from: Liu et. al. [2]).

The first DOP alloy studied extensively was known as DOP-14 and contains the optimal 200 wt-ppm of thorium. It was found that this material had considerable problems with weld solidification cracking and apparently resulted in cracked welds essentially at the 100% level. This was attributed to excessive Th segregation along grain boundaries during solidification. Weld development efforts at that time showed that there was little hope of modifying the weld schedule to eliminate cracking.

Therefore, a second alloy was developed that basically replaced most of the Th with Al. The second alloy has the nominal composition: Ir + 0.3 W + 60 wt-ppm Th + 50 wt-ppm Al. This alloy is known as DOP-26. DOP-26 alloy has become the standard for use in the GPHS program since about 1980.

A Note on the Impact Ductility Test

One of the most important requirements on the GPHS is the performance of its materials in the high strain rate ductility test. Therefore, a brief description of that test will be given here. The details of how the test is actually performed are contained in an ORNL Work Procedure: MET-MatP-SOP-81 Rev. 3. There are important details of how the samples are heat treated, cut and handled but for the purposes of this paper only the basics of the test will be discussed.

The test starts with a 2" blank disc, which is the starting point for drawing of the cup halves. This blank is given the typical recrystallization heat treatment (1350 C / 1 hr) and becomes the starting point for impact testing. It should be noted that the specimens are oriented so that the samples are tested transverse to the rolling direction because that direction tends to yield a bit lower ductility than longitudinal specimens. (Notice that the test specimens are a bit different than the material in the actual clad because they have not been through the forming operation that makes the two cup pieces.) If the intent of the test is to validate weld ductility, a linear weld is then made across the plate. At that point two mini tensile bars are cut from the plate, are given an additional "aging" heat treatment (1500 C / 19 hr) and are loaded into the test fixture. A picture of the test fixture is shown in Figure 3. The essential idea of the test is that a bullet is

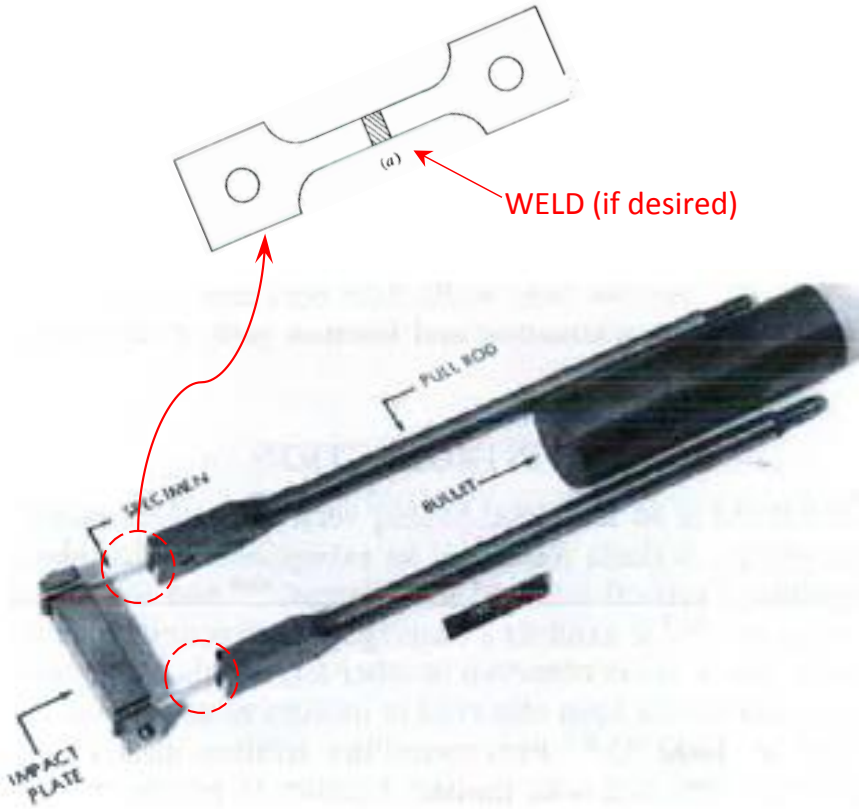

Figure 3: Picture of the impact test fixture and a schematic of the tensile bars.

fired at the impact plate so that the bullet is traveling at 61 m/s upon impact on the impact plate. This tears away the two tensile specimens at a very high strain rate. At that point, a methodology as proscribed by the Work Procedure is used to measure the specimen elongation at the fracture surfaces; those are the high strain rate ductility values discussed in this paper.

A Note on “Old Process” versus “New Process” Material

When considering the literature on DOP-26, a bit of confusion is introduced by the fact that important metal processing changes were made circa 1988. Thus, the nature of these changes and their significance to the weld development efforts will be discussed here.

Serious weld development work on DOP-26 started by about 1980. At that time the DOP-26 was made by melting Ir+Th and Ir+Al master alloy buttons together and making small ingots of roughly 60 g mass. These ingots were of the correct size to make the forming disks. At that point the ingots were rolled to make the forming disks. After a subsequent recrystallization, the formed cup halves were made.

However, this early form of DOP-26 had some serious metallurgical problems. These problems were discussed in Heestand et. al. [3]. In the forming blanks several problems were noted including: lack of homogeneity of the Th distribution; some evidence of pore formation in the base metal and at the grain boundaries; some propensity for near-surface delamination during rolling. Examples of these issues are shown in Figure 4. Additionally, in those early days of iridium fabrication, there is evidence that the overall alloying additions content, specifically of the thorium addition, was relatively poorly controlled. The essential point is that the base metal exhibited problems that probably contributed significantly to welding problems in that material.

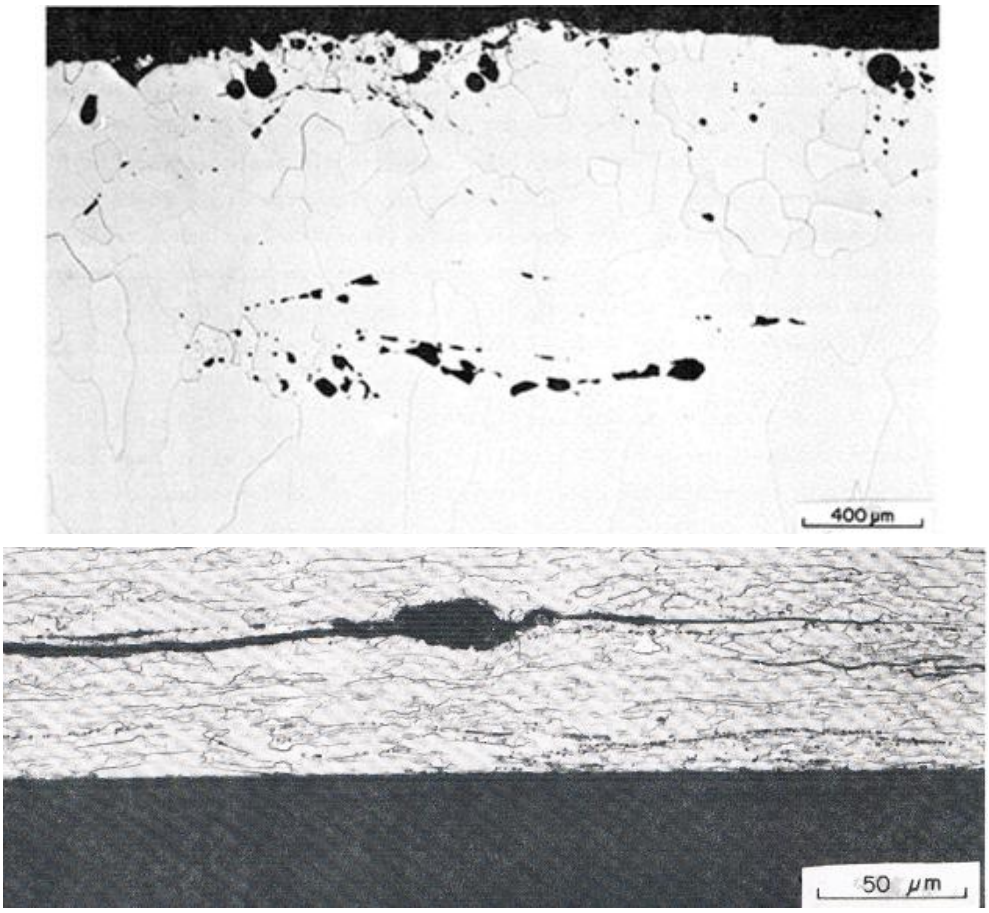

Figure 4: Metallographic sections from DOP-26 rolled plate showing gas voids and near-surface delamination.

Welding problems with this DOP-26 material will be discussed in some detail later in this paper. However, at this time it worth mentioning that the major problem with this DOP-26 material was some tendency for weld solidification cracking. It seems highly likely that this was exacerbated by the gases (and possibly other non-metallic elements) in the base metal. Some corroborating evidence for this assertion was presented by Mosley [4]. In this work, the fracture surfaces resulting from weld solidification cracking were studied with SEM. Figure 5 shows a picture

Figure 5: SEM picture of the fracture surface from a weld solidification crack in the DOP-26. The rounded features are grain boundary cavitation (gas) voids.

of a weld crack fracture surface. One sees ridges that are essentially typical ductile dimpling behavior. However, along these fracture surfaces one tends to find fairly high fractions of the surface area consisting of rounded regions that are clearly gas cavities (as shown in Figure 5). Note that these features are much too small to be seen by the usual RT or UT testing methods. Nevertheless, these low strength/ductility regions along the grain boundaries limit the ductility of the DOP-26 material and clearly contribute to crack formation during welding. Auger electron spectroscopic analysis of the grain boundary cavities suggests that the pressurizing gas contains carbon and calcium and that the cavity forming areas are possibly associated with an elevated Th content (oxygen was not detected – AES does not detect hydrogen). It seems possible that the grain boundary cavities may also be associated with hydrogen. The essential point is that dissolved gases and possibly other tramp elements (such as carbon) were undoubtedly significant contributors to weld solidification cracking in this early DOP-26 material.

The DOP-26 material discussed up to this point has come to be known in the literature as “old process” material. As the weld process development work is discussed in this paper, an effort will be made to distinguish which material was used in that work. This old process material will be designated as DOP26-OP in this paper. Note that any weld development activities accomplished prior to about 1988 are certainly using the DOP26-OP base metal.

Once the issues with dissolved gases and possible alloying element inhomogeneity became apparent, the melting practice for the DOP-26 alloy was substantially modified. These changes are discussed in: Heestand et. al. [3]. The essential change to the processing is that the small ingots resulting from the initial alloying were electron beam melted together to make electrodes for the vacuum arc remelting (VAR) process. VAR resulted in larger starting point ingots for subsequent cutting into smaller pieces followed by the usual rolling. Additionally, any dissolved gases were effectively eliminated from the base metal. VAR material also has the advantage that alloying element content variability throughout the ingot is mostly eliminated. These processing changes were made in about 1988. The resulting DOP-26 base metal is commonly referred to as "new process" material. In this paper that metal will referred to as DOP26-NP. This became the standard base metal after 1988. Note that some legacy DOP26-OP metal may have persisted in the product stream for a while after 1988 but that by 1989 all material studied should be the DOP26-NP.

Some Fundamental Properties of DOP-26

In this section of this paper some of the basic properties of the DOP-26 material (especially as these relate to the high strain rate ductility) will be discussed. These results are presented primarily to give the reader additional background on this material and to present a notion of the development effort that was involved in optimizing the base metal. It is also important to notice that most of the data are high strain rate results (typical strain rates are those from the 61 m/s impact test). It should be immediately made clear that most of these data have little direct connection to the weldability problems seen in DOP-26.

The first basic behavior DOP-26 to be discussed here is the "ductile to brittle" transition. Ductility data from Liu et. al. [2] are shown in Figure 6. This shows that DOP26-OP exhibits a considerable temperature dependence to its high strain rate ductility with higher test temperatures always resulting in higher ductility. Ductility of DOP-26 becomes quite small below about 600 C. This behavior could be relevant to weld solidification cracking because the material becomes quite brittle near to room temperature. However, this does not appear to be particularly relevant to the weld cracking which will be discussed later in this paper. The primary reason for showing Figure 6 is to inform the reader that not all ductility tests as reported in the literature were conducted at the, now standard, test temperature of 980 C. Upon reviewing the literature one can find impact tests performed at a range of temperatures from 650 to 1400 C. In order to properly compare results one must be aware of the large temperature dependence of DOP-26 mechanical behavior.

Another interesting observation relative to iridium is that does exhibit a considerable strain rate dependence. Data excerpted from C.T. Liu and H. Inouye [5] and shown in Figure 7 illustrate this effect for the base Ir-0.3W material. It is interesting that the addition of nominally 30 ppm thorium largely eliminates the strain rate dependence, presumably by stabilizing grain boundaries. These data are presented to once again illustrate that the exact test conditions do have an important effect on the data for high strain rate ductility in these materials.

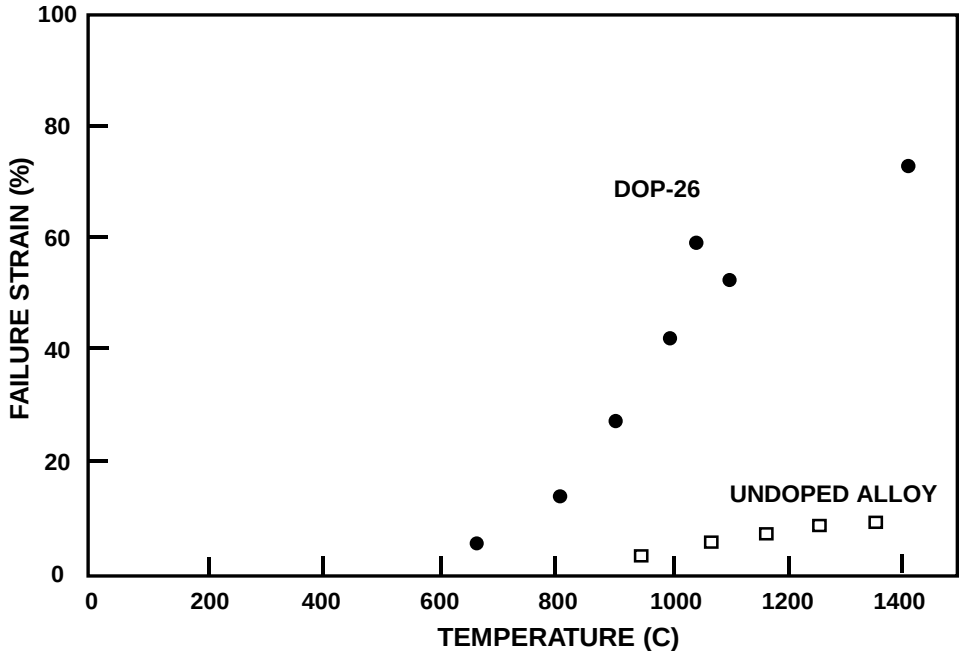

Figure 6: High strain rate ductility of DOP26-OP versus test temperature (from [2]). Also shown are equivalent data points from an alloy containing no thorium that illustrate the considerable improvement in ductility caused by thorium additions.

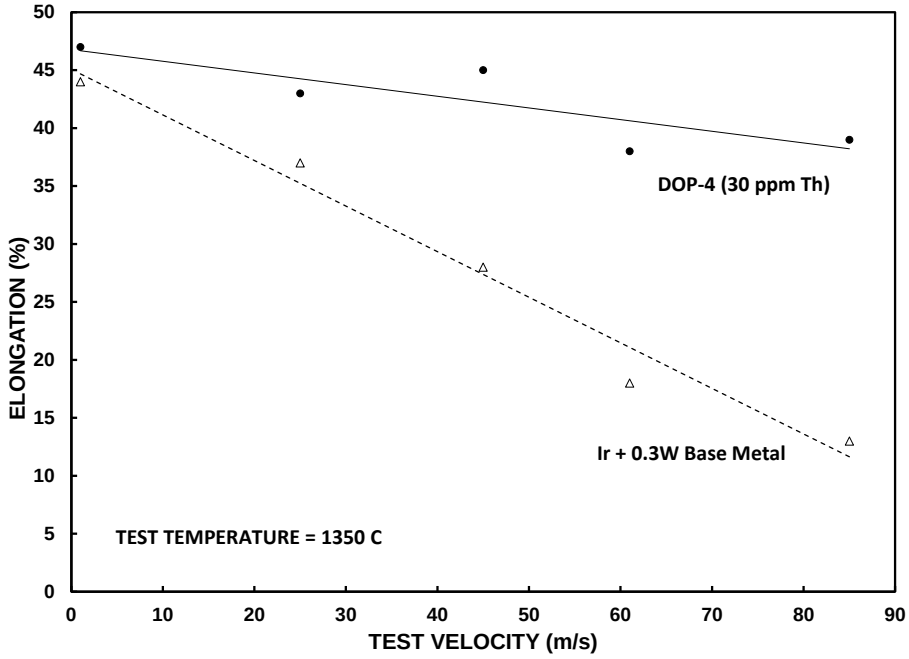

Figure 7: Elongation of iridium alloys in an impact test versus test velocity (from [5]).

Another very important property of the iridium alloys, and that is relevant to welding, is grain size. This is thoroughly discussed in: Liu et. al. [2]. Some data illustrating the grain size effect are shown in Figure 8. As can be seen, there is a large dependence of material ductility on average grain size. These tests were performed at 1350 C and impacted at 85 m/s.

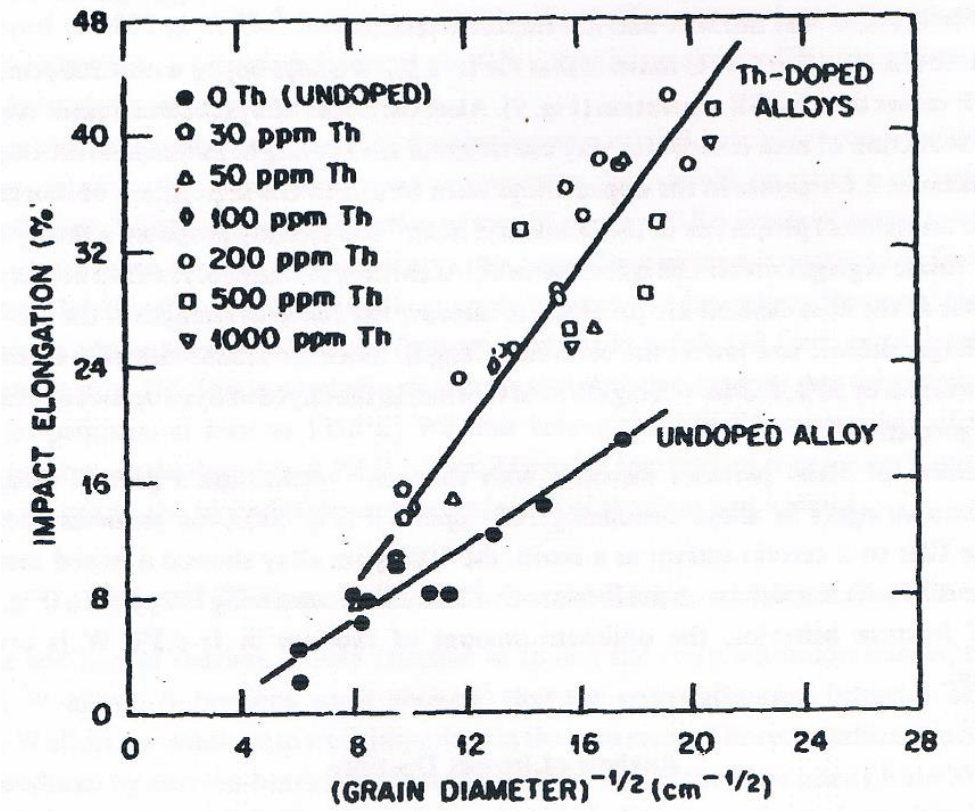

Figure 8: High strain rate ductility of DOP26-OP versus grain size (from [2]).

Theoretical analysis of these data was made assuming that no recovery could occur in this high strain rate test. In that case the critical fracture strain is basically a constant (related to the intrinsic strength of the grain boundaries) plus the usual Griffith criterion for crack expansion. The data in Figure 8 are entirely consistent with this model. There are two important points made by these data. The first is that thorium additions clearly improve the intrinsic strength of the grain boundaries relative to nominally pure iridium. It is interesting to note that there is little systematic difference in the results with small (30 ppm) or large (1000 ppm) thorium addition. The apparent significance of this will be discussed later in this paper. The most critical concept coming from Figure 8 is that the thorium doped material has a large grain size dependence of its high strain rate ductility with coarse grains being considerably deleterious to high strain rate ductility. The same basic point is made by considering data from grain coarsening experiments carried out by: T. George et. al. [1] and shown in Figure 9. In this case the results are correlated to the wall thickness of the GPHS clad. The essential point being that the high strain rate ductility of the DOP26-OP base metal becomes effectively zero if fewer than five grains exist across the wall thickness.

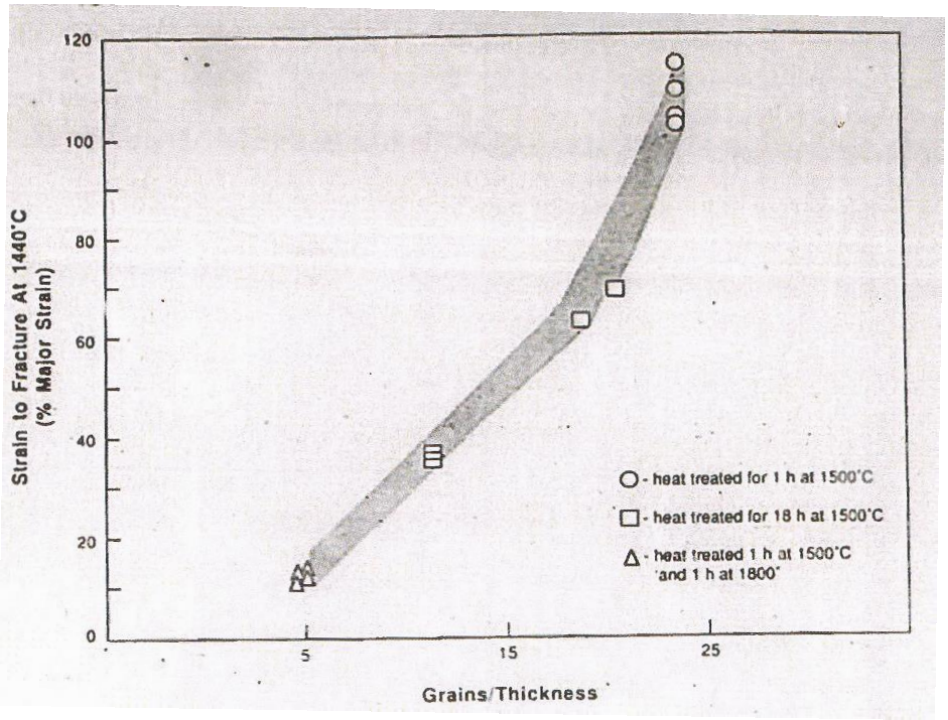

Figure 9: High strain rate ductility of DOP26-OP versus grain size (from [1]).

The significance of these grain size results to welding is that the welding process must be adjusted as well as possible to achieve the minimum possible grain size, especially along the weld center-line. This is also the origin of weld specification requirement for a minimum of six grains along a vertical line through the weld at the weld center-line (with no single grain being greater than 50% of the wall thickness).

An important issue for welding is the possible effect of minor alloy contaminants on metal properties especially as this might relate to the formation of complex intermetallics (that could exhibit brittle behavior). Studies of this possibility have been performed and some basic data on this issue are presented in C.G. McKamey et. al. [6]. Some of these data are shown in Figure 10. The essential result from those studies is that small amounts of those elements have little effect on the base metal high strain rate ductility. Some limited interaction of some of these elements with thorium have been noted (presumably as a result of formation of various complex intermetallics at the grain boundaries). Figure 10 does show an important decrease in high strain rate ductility with silicon additions to the iridium, which apparently occurs largely because the silicon tends to force the thorium off the grain boundaries. However, it should be noted that the DOP-26 certification specifications limit the contents of these tramp elements. Most are specified to be below the 50 wt-ppm level (up to 150 wt-ppm of Fe is allowed) where their effects should be negligible. Additionally, since the effect of gaseous elements as well as possibly carbon and calcium is known to be important, the content of the base metal for these non-metallic impurities is also limited to be below 50 wt-ppm. It does seem that minor element effects in DOP26-NP should be unimportant. However, it is important to note that the chemistry control on DOP26-OP may not have been as good as it is now (for example the actual Th content of the material probably varied by at least +/- 50% for the DOP26-OP material).

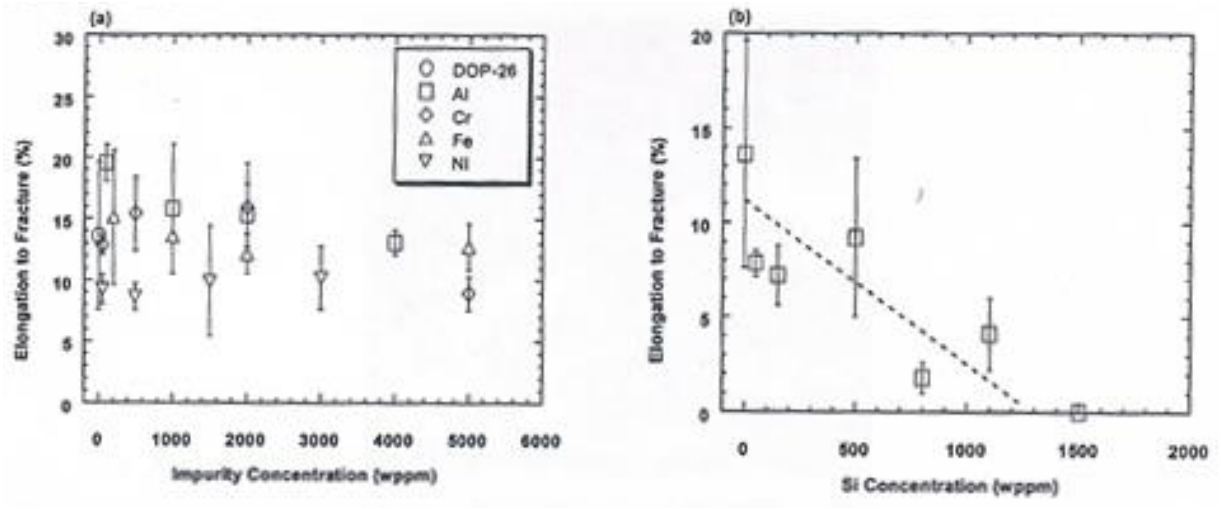

Figure 10: High strain rate ductility of DOP26-OP versus the content of various tramp elements (from [6]).

Another DOP26-NP base metal behavior that might be important to welding behavior is that the base metal behavior continues to have at least some sensitivity to the details of processing. High strain data from 30 lots of material (total of 98 data points) was provided to us by Miller [7]. There is variability in the data within results from any lot of material, presumably as a result of the inevitable uncertainty in any failure measurement. It appears that the experimental uncertainty of any particular data point is about: $\Delta \varepsilon$ = +/- 2%. Combining these results as shown in Figure 11, the production process presently seems to be yielding an average high strain rate ductility of about 23 +/- 5% (the 5% standard deviation is an estimate of uncertainty in the process yield made by noticing that the process yield approximately followed a typical normal distribution behavior). This value of normal distribution width is consistent with base metal average grain size varying between about 40 – 60 um (possible normal variations in other factors such as alloy composition may also contribute to this alloy variability). It does appear that base metal processing is under control and unlikely to be a significant contributor to any welding problems. However, the significance of this to welding is that high strain specimens cut from welded specimens seem to have a high strain rate elongation that is related to the elongation of the base metal (the welded sections typically exhibit elongation that is roughly one-half of the base metal value). This suggests that details of the base material (possible Th content variability, grain size and etc.) could be important to weld performance. We do not presently have similar process yield data for DOP26-OP. However, based on historical data relative to high strain rate ductility, the performance of DOP26-OP must have been similar.

Failure analysis calculations for the GPHS showed that the capsules would have a good chance of surviving an accident if the DOP-26 base metal has an impact ductility greater than 13.5%. Therefore, that is the minimum value allowed for the base metal. Data such as that shown in Figure 11 indicate that the recently manufactured DOP26-NP base metal should always be safely above that minimum level.

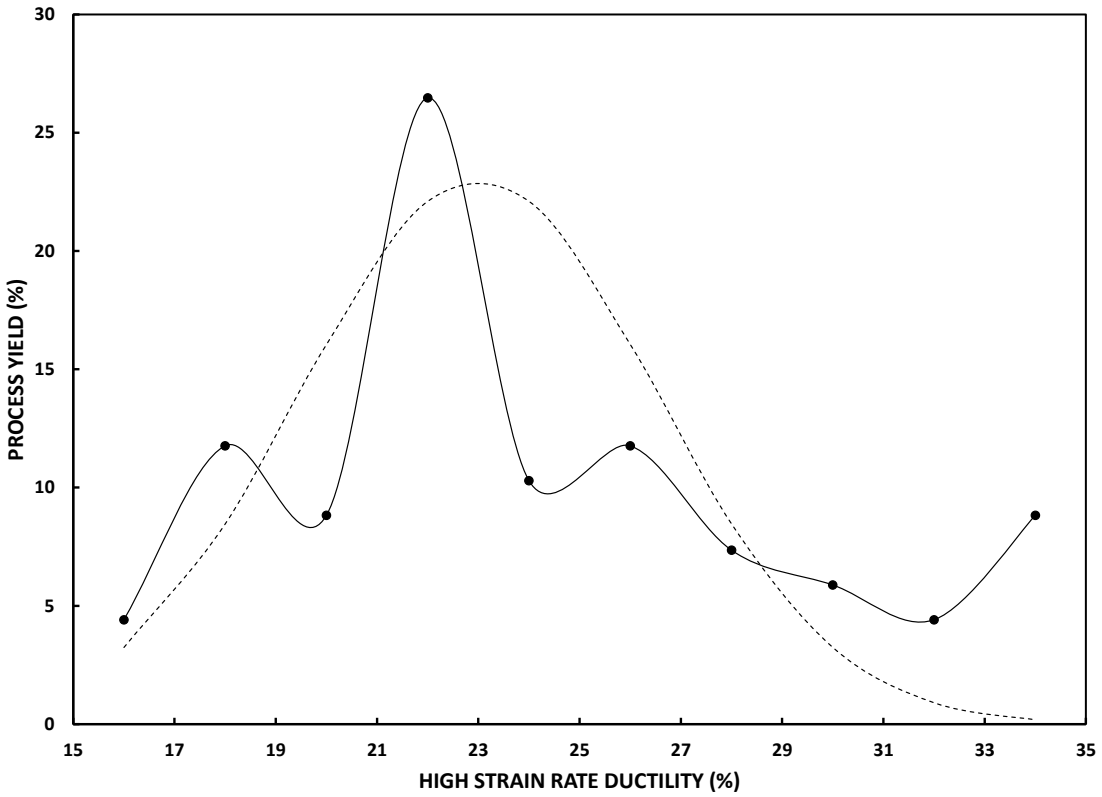

Figure 11: Process yield (in percent of total product) versus resulting high strain rate ductility for a number of recent lots of DOP26-NP (from [6]). The dashed line is a least-squares fit to the data assuming that the process yield approximately follows a normal distribution, which indicates that the process is yielding: $\varepsilon = 23 +/- 5$ %.

Welded metal typically has considerably lower high strain rate elongation (some possible reasons for this will be discussed later as the welding is discussed) that does seem to correlate at least in a general way with the base metal properties (weld metal ductility generally being roughly ½ the base metal value). The most important goal of weld development is to achieve weld properties as near to the base metal value as possible.

THE ROLE OF THORIUM IN IRIDIUM ALLOYS

To start this presentation of the effects of thorium in the DOP alloys, the Ir + Th phase diagram will be considered. An ASM binary phase diagram for this system is shown in Figure 12.

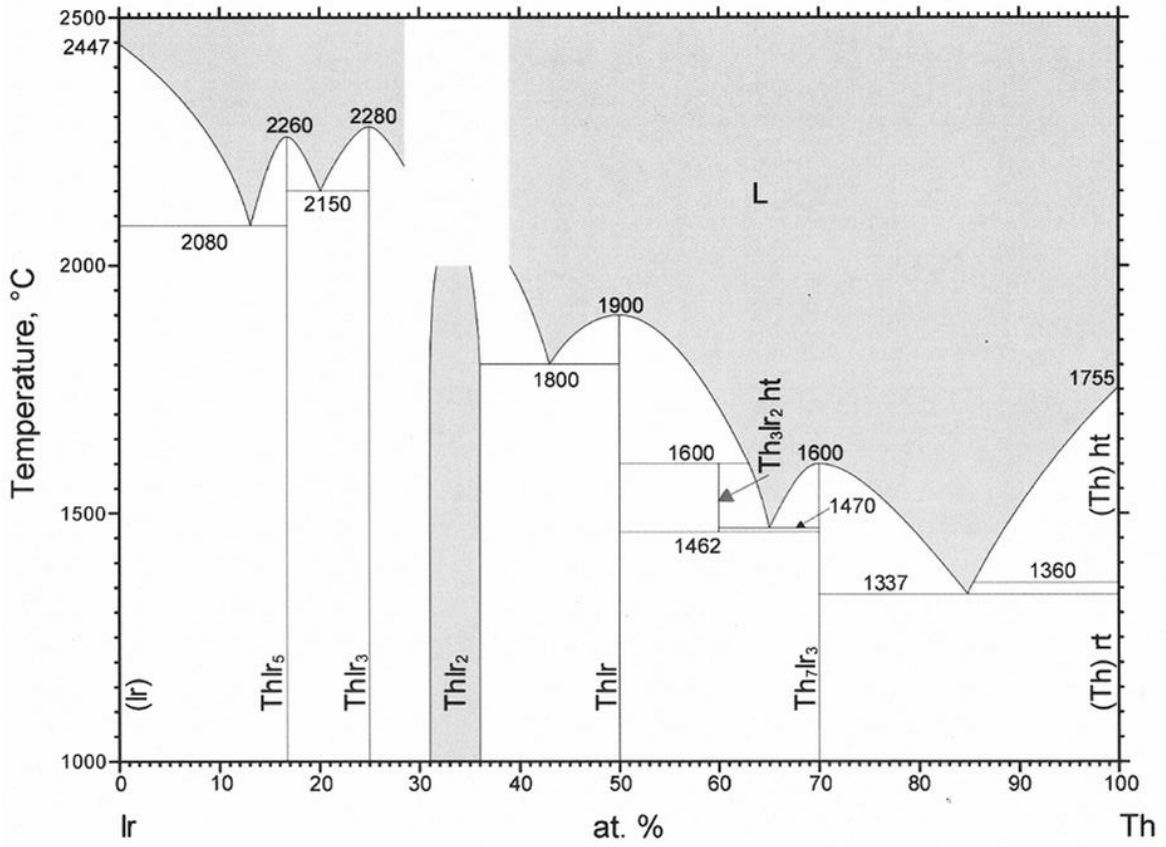

Figure 12: Binary phase diagram for Ir + Th from: ASM International, “Binary Phase Diagrams”.

Unfortunately, the diagram is a bit incomplete because it does not expand on the very low thorium content portion of the diagram. Specifically, the solid solubility of Th in Ir is not presented. Apparently, this value has not been directly measured. However as will be discussed subsequently, the actually solubility of Th in Ir is clearly quite limited and is probably roughly 5 at-ppm. The particularly relevant features of this phase diagram at the low thorium content end are the presence of a eutectic (with nominal composition of about Ir + 13 a/o Th) with its low melting point and the existence of an Ir_5Th intermetallic.

The significance of the low solid solubility of thorium in iridium is that the Th will tend to segregate from the solidifying material as the (presumably properly homogeneous) melt starts to cool and solidify. This means that, for some distance (basically limited by a diffusional process) ahead of the solidification front, the Th content of the fluid becomes considerably elevated. This excess Th tends to get dumped at grain boundaries. Thus, the grain boundary Th content will be greatly above that of the nominal alloy content. Since there is a considerable thermodynamic driving force for formation of the eutectic and of the Ir_5Th intermetallic, the grain boundaries in the solid will tend to contain these structures. Presumably, the eutectic is largely

responsible for the greater grain boundary cohesion seen in the DOP 14 and 26 alloys. Additionally, particulate of the Th Ir_5 intermetallic at the grain boundaries will tend to pin those boundaries and improve the high strain rate ductility of the alloy. Thus, the primary effect of Th in the DOP alloys is a result of its considerable tendency to reside at the grain boundaries in the solid and to thus improve the mechanical properties of that material.

Some data illustrating the considerable thorium segregation to grain boundaries are presented in Heatherly and George [8]. They performed microprobe Auger electron analysis of metallic impurities in the Ir and specifically in the grain boundary regions. The basic result from this work is that, in the DOP-26 base metal, the Th content at grain boundaries is an average of about 6 at-% and is basically undetectable in the transgranular regions. Thorium content detected in the grain boundaries varied considerably over a range of about 2 – 10 at-%. Their data imply that the Th solid solubility is in the neighborhood of 5-10 at-ppm. These results show the large tendency for thorium segregation and confirm that the thorium content of the grain boundaries rises to a level consistent with formation of the eutectic and of the Ir_5Th intermetallic.

Unfortunately, the exact reasons why Th is beneficial to the mechanical properties of the base metal are also the reasons why welding of this material can be problematic. The basic point is that the thorium will be strongly segregated to the weld metal grain boundaries during solidification. In that case the eutectic reaction can occur: L <-> (Ir) + Ir_5Th at 2080 C. This is accompanied by congruent melting of the Ir_5Th at 2260 C. Since these melting points are significantly below the melting point of iridium (2447 C), grain boundary strength in the solid can be effectively zero at temperatures significantly below the melting point; especially if sufficient Th is available that grain boundaries consist of an essentially continuous layer of the eutectic. This will create a high propensity for weld solidification cracking if the stress levels around the weld are high enough. Further illustrating this point about the eutectic formation at the grain boundaries is an SEM picture, shown in Figure 13, of an arc weld fracture surface in DOP26-OP from: David and Liu [9]. This SEM picture clearly shows a patch of the Ir + Ir_5Th eutectic covering much of that fracture face.

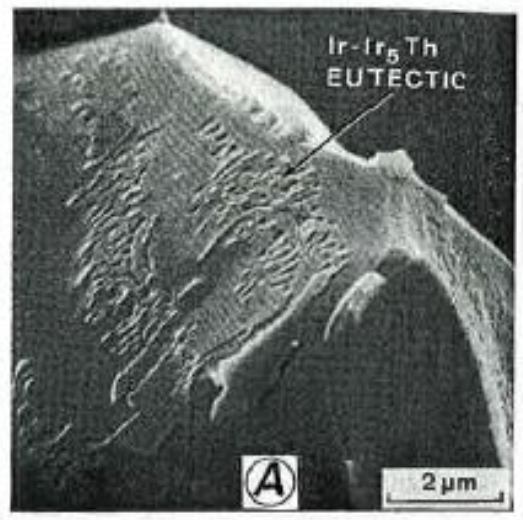

Figure 13: SEM picture of an arc weld fracture surface in DOP26-OP material showing the Ir + Ir_5Th eutectic (from [9]).

An additional point about the significance of thorium segregation to grain boundaries must be made. The actual thorium content at the base metal grain boundaries is inevitably less than in the weld metal because properly produced DOP-26 base metal has much smaller grain size (an equivalent amount of thorium distributed over multiple grain boundaries). Thorium grain boundary concentrations have been made by several researchers and the results vary considerably. This is probably a testament to the fact that this is a difficult measurement. It appears that thorium contents in grain boundaries of the base metal is probably about 5 wt-% while it can be as high as perhaps 20 wt-% in weld metal. In any case, grain boundary liquation in the HAZ of the base metal is also a possibility for the same reasons that weld metal cracking is likely. The essential point is that, depending on the details of cooling stress as it develops around the weld, it is possible for cracks to develop in the HAZ and possibly propagate further into the base metal and/or into the weld metal.

SOME CONSIDERATIONS FOR WELDING

Strictly from the viewpoint of welding, the primary concern with GTA welding of DOP-26 is its tendency for weld solidification cracking. The data presented up to this point in this paper are mostly high strain rate ductility data. While there is undoubtedly some connection between these results and base metal quality factors that could affect weld cracking, generally these data are of limited value for understanding weld cracking for several reasons. One important factor is that the impact tests are performed at temperatures considerably below the base metal melting point and, therefore, these data do not address the temperature range where weld cracking initiates. Another interesting problem with the impact test is that the specimens being prepared for the test are given an aging heat treatment (in various publications different heat treatments have been used, varying between about 1300 and 1500 C with durations ranging from 1 to at least 19 hours). This is equivalent to a post-weld-heat-treatment that can change the weld metal properties considerably through a variety of factors such as: grain coarsening, alloying element redistribution, relaxation of residual stress and etc.

The essential point is that the impact test results, while important indicators of the ultimate serviceability of the welded assembly, are not particularly relevant to the issue of weld cracking. Therefore, an additional mechanical testing method was required for weld development work. The alternative method chosen for application to GPHS weld development is known as the Sigmajig test method. Some additional data were obtained with a circular patch test.

Mechanical Testing for Weld Cracking Susceptibility - Sigmajig

The Sigmajig test was developed by Goodwin [10] as a simple test of the relative weldability of hot cracking susceptible materials. The basic idea is to clamp a thin piece of the material in a fixture and use spring tension to place the sheet in a uniform transverse stress. With appropriately calibrated springs, the initial stress state of the material is known. At that point a linear weld (can be any welding process but it is GTAW in this case) using the appropriate weld variables is made down the middle of the exposed sheet. The specimen is then inspected for the presence of center-line cracking. By making multiple tests with increasing initial stress the threshold stress for cracking behavior can be simply established.

It is possible to use the Sigmajig data in several ways. For example, it is possible to count total crack length at a particular stress level with total crack length being correlated to material hot cracking susceptibility. An additional bit of data that can be derived from the test is to measure the reduction-in-area seen in a failed specimen. For the purposes of this paper, the Sigmajig has basically been used to identify the threshold stress for cracking behavior, ie. the initial stress value where significant center-line weld cracking is seen. The higher the initial stress at the onset of cracking, the better the material and weld schedule combination is performing relative to weld solidification cracking behavior.

An important complication relative to Sigmajig results must be mentioned. It is effectively impossible to correlate Sigmajig data with conventional mechanical testing data. This is so because the actual stress on the weld area is quite dynamic. As the heat source approaches a spot on the plate the resulting thermal expansion causes the transverse stress to decrease to a fraction of the initial load. After the heat source passes the material cools and contracts and the load relatively slowly recovers to the initial transverse stress (final stress will be a bit different than the initial applied load depending on the degree of material cracking and its high temperature ductility). Because of this dynamic loading, Sigmajig results should be considered a "screening test" for relative material weldability.

Some Basic Sigmajig Test Results for DOP-26

An example of the usefulness of the Sigmajig test is presented in: David et. al. [11]. The resulting data are summarized in Figure 14. This shows the threshold cracking stress of

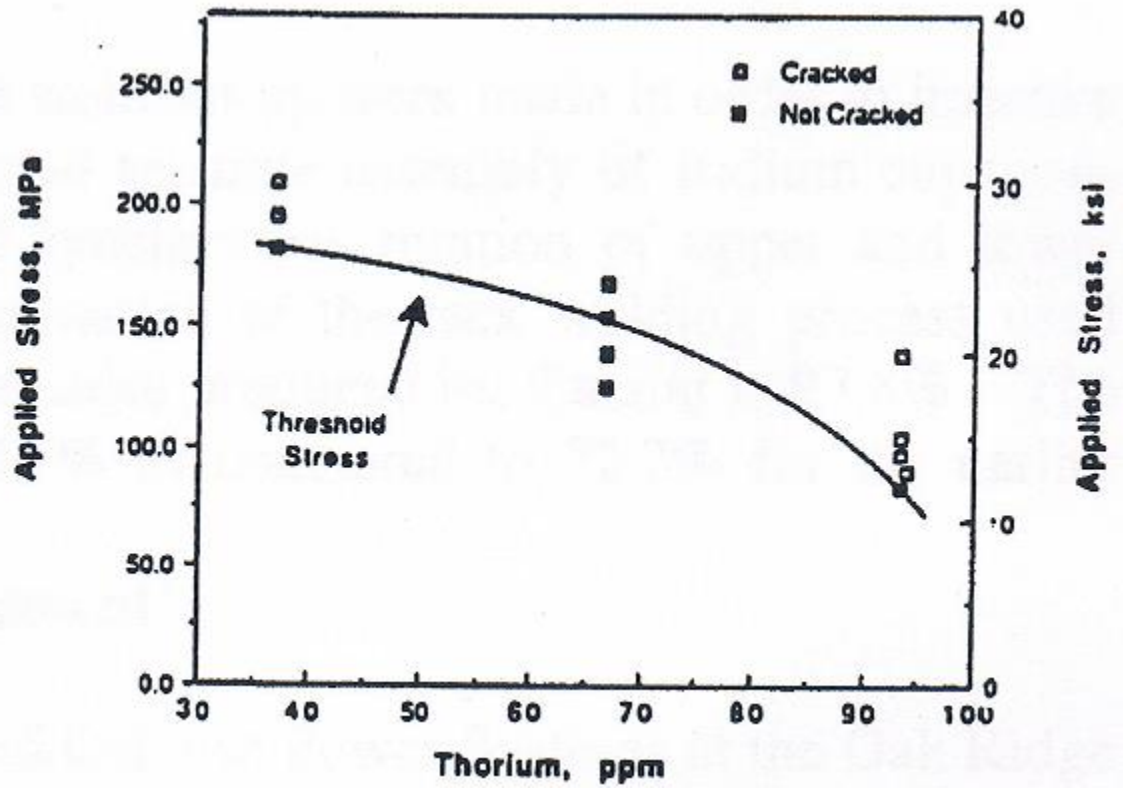

Figure 14: Sigmajig threshold stress for a typical GTA weld on "old process" DOP alloys versus alloy thorium content (from [11]).

iridium + thorium alloys versus thorium level. (To put the Sigmajig threshold cracking stress values in perspective, it is interesting to note that these values for < 60 ppm thorium are about the same as Type 316 stainless steel, when welded at similar travel speed. This stainless steel has some propensity for cracking but can be welded without the need for extraordinary measures.) As can be seen, the threshold cracking stress of the iridium alloy decreases by about 50% as the thorium content is increased from 30 to 100 ppm. Extrapolation of the curve shown on Figure 14 indicates that an alloy containing 200 ppm of thorium (such as the original DOP-14) would have very high cracking susceptibility. Of course, this is consistent with the observation that the 200 ppm thorium alloy is not readily weldable. The data shown in Figure 14 are basically the reason that the nominal thorium content of DOP-26 (60 ppm) was chosen. The DOP-26 composition is a compromise between optimal impact ductility and reasonable hot-cracking susceptibility. This illustrates the utility of a weldability test such as the Sigmajig.

Some additional interesting data illustrating the usefulness of the Sigmajig test are presented in: Goodwin and Ohriner [12]. Since late 1989 all heats of DOP-26 iridium alloy have routinely been evaluated for weldability using the Sigmajig test. This particular Sigmajig test makes a typical GTA weld using 125 A of weld current at a travel speed of 12.7 mm/s in a glove box filled with pure argon gas (note, no arc oscillation is typical). In the course of this routine testing other material factors were considered, such as “old” versus “new” process material and the potential for recycling the iridium by remelting. The summary data from that report are presented in Figure 15. There are several features of that data that are noteworthy.

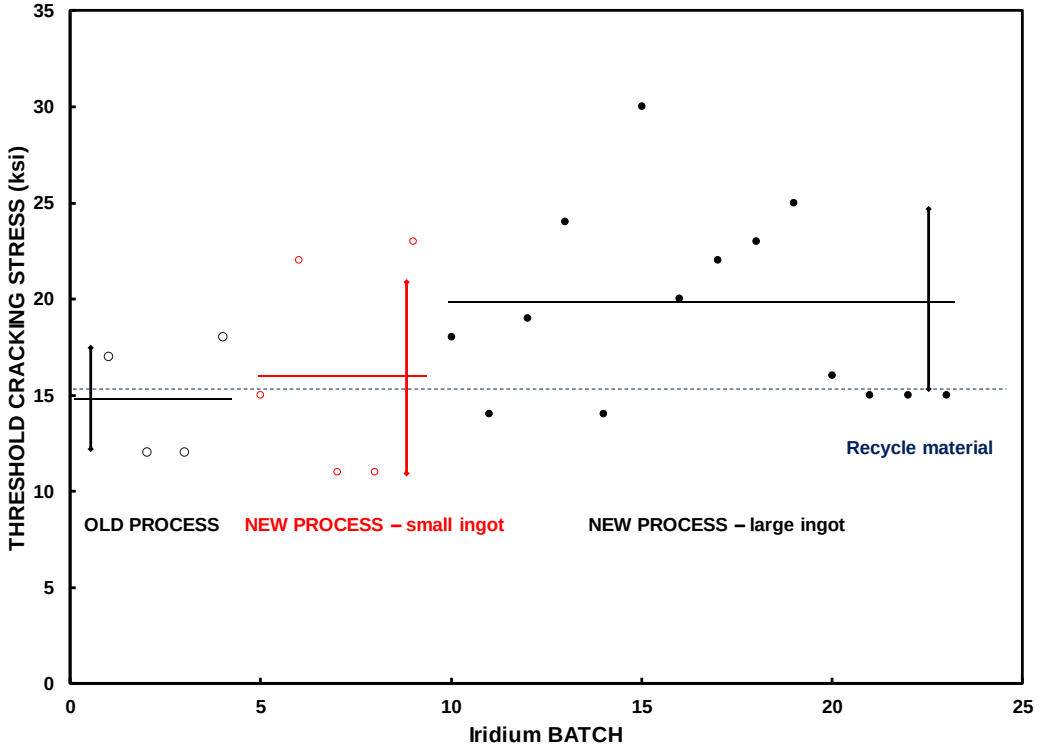

Figure 15: Sigmajig threshold stress for a typical GTA weld on DOP-26 (from [12]). The figure includes data from old process and new process material (produced with two different ingot sizes). The horizontal dashed line shows the average value determined for recycled material. The vertical lines are the standard deviation of the results for that material condition.

The first interesting feature of these data is that the more recent DOP26-NP material shows about a 30% greater threshold cracking stress than DOP26-OP. Of course, these data must be approached with a bit of caution since only a limited number of data points are shown for any material type. Further, when one considers the standard deviation in all of the measurements, it is not apparent that the DOP26-OP and DOP26-NP results are actually statistically different. (Of course, the large standard deviation of the DOP26-NP results is also somewhat concerning and may suggest that even the DOP26-NP may have important variability problems.) Nevertheless, it does appear that the VAR processing of DOP-26 did improve its weldability. This is certainly supporting information suggesting that welding process development work, largely having been performed on DOP26-OP material, could be revisited on DOP26-NP.

Two other interesting things are shown in Figure 15. The DOP26-NP results are presented in two groups. The first group is labeled “new process – small ingot”. When the VAR processing was first introduced the resulting ingots used for the forming operation were 51 mm in diameter and were just adequate in size for the subsequent rolling and forming of cups. Later the ingot size was increased to 63 mm diameter resulting in a forming blank with significant discarded material. Sigmajig results for that material are labeled as “new process – large ingot”. Interestingly, it appears that much of the difference between DOP26-OP and DOP26-NP is not just a result of the VAR processing of the material. An additional (and probably related phenomenon) is suggested by the horizontal line on Figure 15, which is the average Sigmajig result for recycled material. The basic idea for recycling is that GPHS blank fabrication results in considerable scrap of the expensive iridium material and that it would be highly advantageous if that material could be recycled. Sigmajig tests on remelted scrap show properties consistent with the DOP26-OP material. The apparent significance of the dependence on recycling and on ingot size is that DOP-26 weldability is sensitive to pickup of non-metallic impurities and possibly on alloying element loss during processing. The sensitivity of DOP-26 to processing details, and especially to the potential for impurity pickup during processing, is clearly critical to welding success and should be considered during weld development and production activities.

Some additional interesting information resulting from the routine Sigmajig testing was presented by Ohriner et. al. [13]. Since the Sigmajig testing is done in a glove box (apparently with no additional shielding gas) some data were collected to investigate the possibility of oxygen pickup during welding having an effect on the data. Figure 16 shows threshold cracking stress for DOP-26 with the glove box atmosphere containing up to 2000 ppm oxygen. As can be seen, this had no effect on the weld metal cracking behavior. Similar experiments with water vapor contamination showed similar results. Also shown on Figure 16 is another interesting aspect of these data; a considerable increase in weld width with oxygen addition. The description of weld appearance accompanying these results [13] strongly suggests that the oxygen addition substantially decreased the surface tension of the liquid metal (a common result for most “pure” metals). The significant weld shape change is qualitatively similar to that produced by Marangoni flow in the weld metal (although in general, modest oxygen additions would result in a deeper weld – this general observation is known to be complicated in thin material). The other important point is that the significant increase in weld width had no measureable effect on weld cracking susceptibility. This is another bit of evidence that cracking may be less dependent on weld shape in DOP26-NP material than was previously observed.

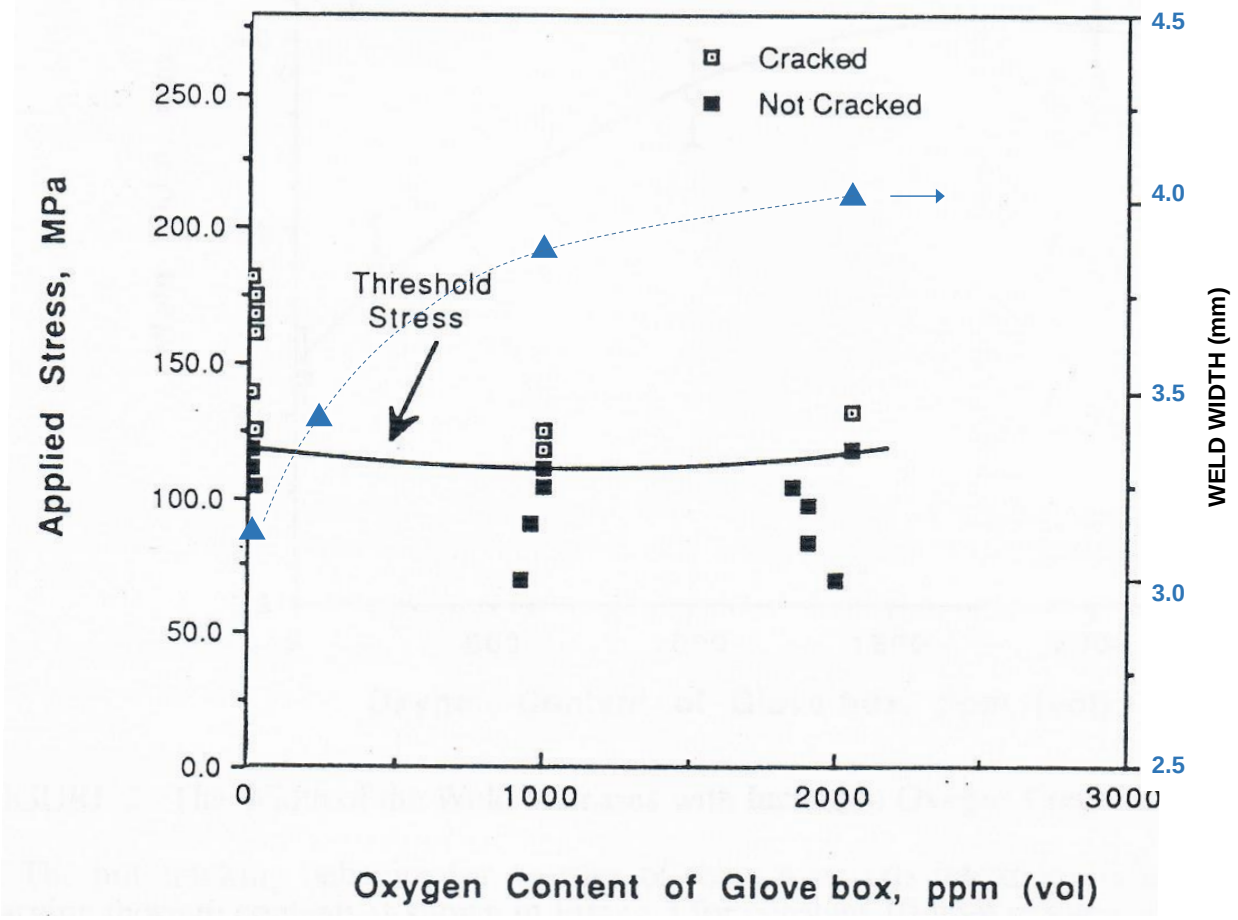

Figure 16: Sigmajig threshold stress for a typical GTA weld on DOP26-NP versus oxygen content of the argon in the glovebox (from [13]). Also included on the figure are measured weld widths (secondary axis) for similar argon oxygen contents.

Base Metal Weldability of DOP-26 – Modified Circular Patch Test

Some additional useful data relative to DOP-26 weldability was presented by: David and Woodhouse [14]. In this test, welds are made around a closed circle on thin pieces of the test material. The arc welds were made with the usual Sigmajig weld variables and did include transverse arc oscillation. The test procedure was to first make a weld on the plate having a circle diameter of 1.375" and then to follow that with an inner circle with a diameter of 0.875". The inner circle represents a considerably higher degree of weld restraint (resulting higher stress) and is, therefore, a more stringent test of cracking susceptibility. Prior to testing the material thorium contents were determined by: 1. Spark source mass spectography; 2. Isotope dilution mass spectography (in general the two results were similar but the isotope dilution mass spectography values tended to be about 25% higher).

In order to present the David and Woodhouse [14] data in a graphical form, a cracking index value was assigned to the cracking observations. In this case: -1 represents no cracking; +1 is observed cracking only on the small diameter circle; +2 is observed cracking on the large diameter circle. The results of analyzing the data in this way are shown in Figure 17.

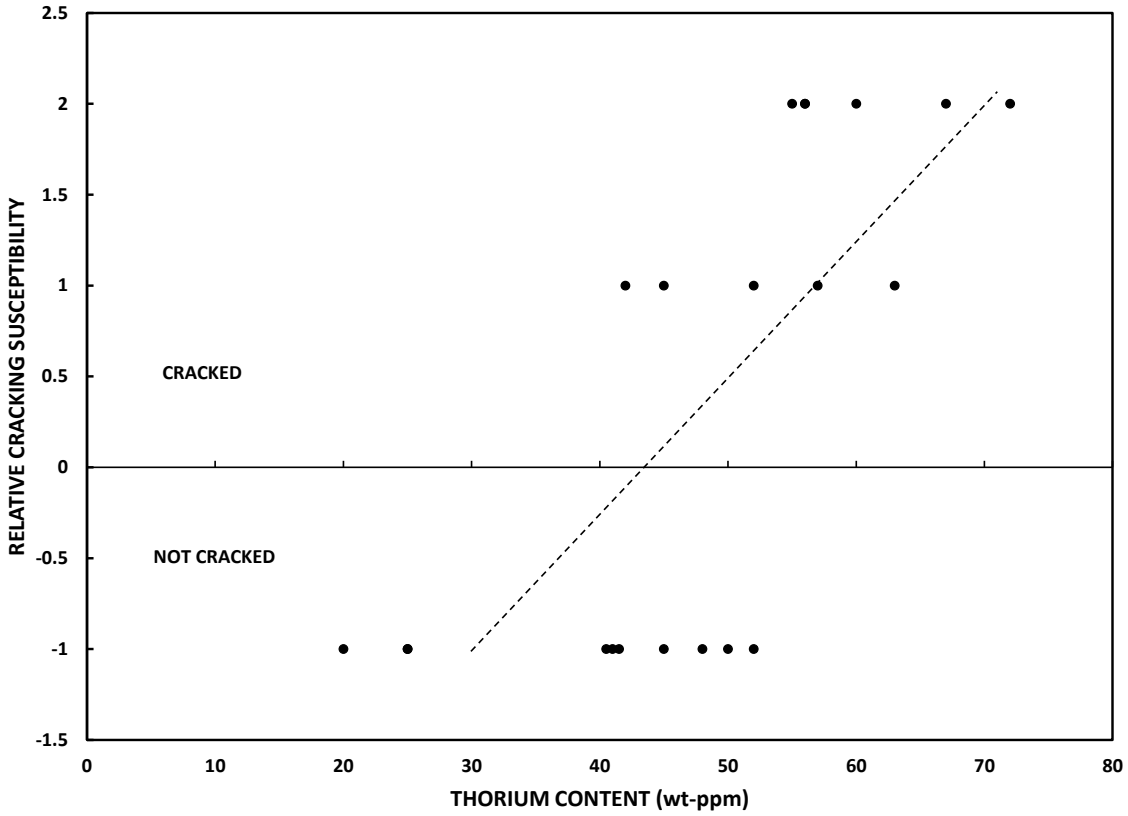

Figure 17: Relative cracking susceptibility of DOP26-OP in a circular patch test versus base metal thorium content (from [14]).

This test was performed on 21 material samples from a number of different batches of the DOP26-OP material. The essential result from this circular patch test is that cracking susceptibility of the base metal is minimal below about 50 wt-ppm thorium content and gets significantly worse for thorium contents above that value. This is in agreement with the Sigmajig test results shown in Figure 14. Cracking susceptibility of the material is good for low thorium contents, generally those below 50 wt-ppm of thorium, and basically doubles as the thorium content increases above 100 wt-ppm. These data further reinforce the point that the thorium content of "old process" DOP-26 was variable and that the actual base metal thorium content could easily be in the range where material weld solidification cracking is a major problem. The data of David and Woodhouse show that roughly 25% of the material batches had thorium contents high enough to cause cracking susceptibility. It is interesting to note that this is entirely consistent with the cracking failure rate which was seen in production welding using this material (the production welding issue will be discussed later in this paper).

BASIC WELD DEVELOPMENT CONSIDERATIONS

This section of this paper is dedicated to a literature review of weld development for DOP-26 with an accent on grain growth modification and on the hot cracking tendency of the material. An additional important goal of this section is to discuss the effects of magnetic arc oscillation (MAO) finally used in the GTAW process for GPHS fabrication. MAO clearly made a significant improvement to the process on DOP26-OP but it is somewhat unclear as to whether this is now an essential ingredient of the GTAW process.

Some of the first studies of iridium welding were associated with encapsulation of a source similar to the GPHS but with a wall thickness of about 0.6 mm. This early work by Coffey et. al. [15] indicated that the nominally pure iridium is readily weldable with GTAW. However, the material did tend to fail in impact, vibration and shock testing. As is typical of pure metals, the base metal and the weld had a coarse grain structure. Grain size in this material was on the order of 100 microns with many grains of about 300 microns, which means that this material would have intrinsically low impact ductility. Weld metal tended to have worse properties from the viewpoint of impact ductility. For example, they reported essentially a single columnar grain at the weld center-line in welds made at low travel speed of 5 mm/s. An example of this grain structure is shown in Figure 18. The grain structure along the weld center-line consisted of

Figure 18: Photo of the weld center-line microstructure of a typical GTA weld in iridium. Note the essentially continuous single grain boundaries oriented vertically in the section. The weld was made at travel speed of 5 mm/s (12 ipm).

essentially single grain boundaries extending through the part thickness. This structure is particularly susceptible to fracture. Better weld grain structure was obtained at a higher travel speed of 12.7 mm/s with multiple grains resulting in the thickness direction. They also reported substantial grain refinement using 6.25 Hz arc oscillation. The “optimized” weld obtained in this study of optimally pure iridium is shown in Figure 19. Viewed objectively, it is not obvious that considerable weld improvement resulted from the recommended process changes.

These results are not particularly relevant to DOP-26 welding but are mentioned because the lessons learned on pure iridium clearly drove much of the weld development philosophy that followed. Welding at a travel speed of 12.7 mm/s with arc oscillation (quantitative details of the arc oscillation are not known) became the starting point for much of the ensuing weld development activities on the DOP alloys.

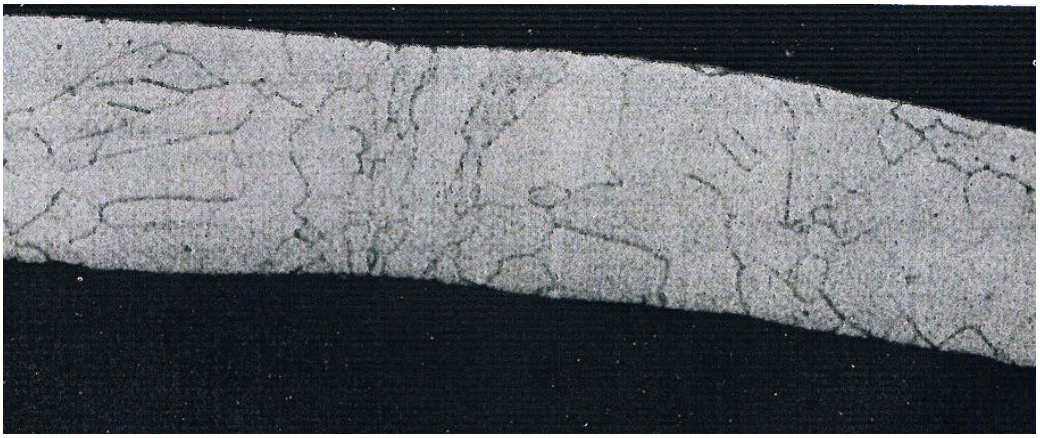

Figure 19: Photo of the weld center-line microstructure of a GTA weld on iridium. The weld was made at travel speed of 12.7 mm/s and with arc oscillation.

The initial weld results made it clear that nominally pure iridium had unacceptable impact properties and, therefore, studies of the DOP series of alloys were undertaken. As discussed earlier, the baseline for further development was the Ir + 0.3W alloy. Early weld development on this series of materials was performed by David and Liu [16]. This work looked primarily at EBW because the important weld parameters in EBW are well-controlled and the weld size can be systematically changed by using beam defocus. These results were basically a screening test of the viability of various thorium and aluminum levels on DOP alloy weldability. The basic result of the study was that any of the DOP alloys with thorium content greater than 100 ppm exhibited cracking susceptibility in both the GTAW and EBW processes and that for less than 100 ppm thorium the iridium was weldable with minimal cracking susceptibility.

The majority of the David and Liu [16] initial welding studies was EBW on 200 ppm Th material. (It should be noted that these studies did use material made with “old process” melting practice. It is possible that similar studies on “new process” material may yield a bit different results.) The basic results from this study can be summarized as: 1) weldability was very sensitive to welding speed; 2) weldability was sensitive to FZ width. Their basic result on travel speed is that crack formation was quite prevalent at low welding speed (2.5 mm/s) and that the range of acceptable (lack of cracking) welds increased with increasing travel speed. The speed dependence is apparently mostly a result of grain growth direction and resulting overall grain size. The FZ width dependence is probably a combination of three factors: 1. a wider weld has more thorium available to be segregated to grain boundaries; 2. wider welds will inevitably have different temperature gradients relative to the cooling rate (hence, modifying grain growth behavior); 3. cooling stresses associated with the wider welds will be greater. The data from David and Liu [9] and [16] show that the DOP-14 alloy is weldable by the high energy density processes, EBW and LBW, at typical travel speeds (> 10 mm/s) but with fairly narrow bead width. For example: the alloy with 200 ppm Th + 60 ppm Al showed good EBW weldability at a travel speed of 12.7 mm/s and with a bead width of about 1.5 mm. The laser welds seemed to show that weld widths up to perhaps 2.4 mm (this is top surface width; bottom surface width was about 1.6 mm) are crack free. Arc welds, with the considerably greater FZ width and greater thorium segregation in the weld metal grain boundaries, inevitably cracked in the DOP-14 type alloys.

One of the important observations from the David and Liu papers is the details of the cracking behavior. In the series of > 200 ppm thorium alloys, the considerable cracking sensitivity did appear to be center-line cracks consistent with the typical concepts of solidification cracking. However, careful examination of the cracks showed that most actually initiated in the HAZ and propagated out into the weld metal and then turned to follow the weld center-line. An example of this behavior is shown in Figure 20. These cracks occurred near the weld start and apparently initiated as liquation cracks in the HAZ (base metal) grain boundaries and the fracture followed partially solidified weld metal grain boundaries out into the body of the weld and along the weld center-line This suggests that the details of thorium segregation to grain boundaries in the base metal as well as in the weld metal is probably of critical importance to weldability.

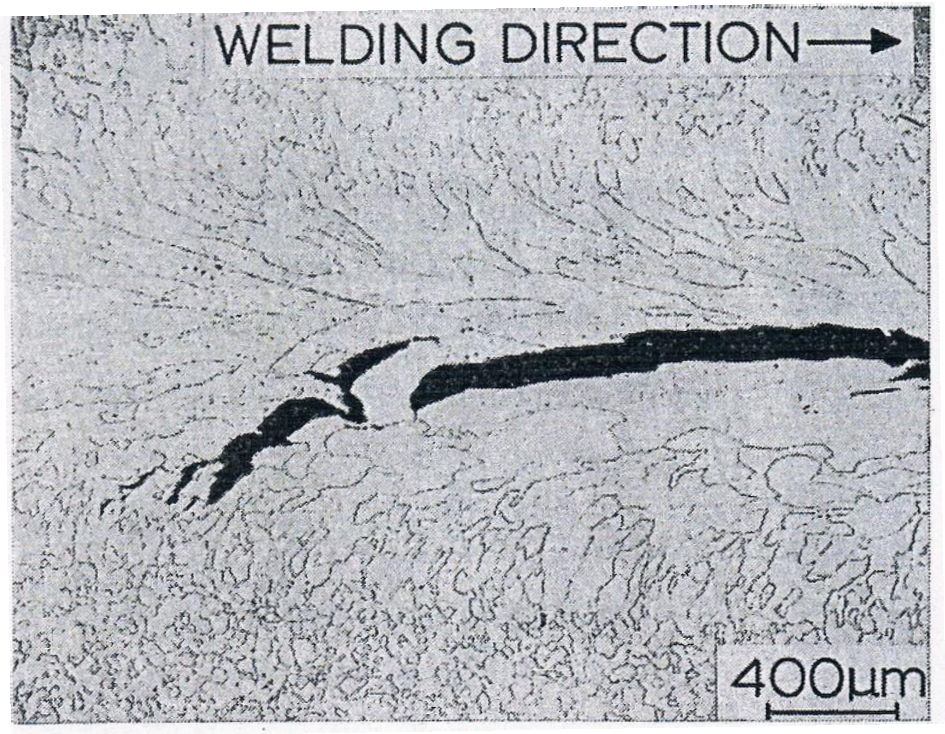

Figure 20: Photo of the weld top surface from a cracked EBW on iridium + 200 ppm Th alloy. Notice that the crack does seem to initiate on liquated base metal grain boundaries.

After these initial weldability studies made it clear that the > 200 ppm thorium had considerable tendency to weld solidification cracking, DOP-26 became the baseline material. The welding studies moved towards optimizing DOP-26 welding. Since there was apparently minimal concern with weld solidification cracking in DOP-26, the fundamental concern for weld development became optimizing grain structure to produce the best possible impact ductility of the weldment. Referencing Figure 6 for example, weldment optimization consists of producing the minimum grain size to ensure that the weld metal consists of multiple interlocking grains in any direction within the weld metal.

Some Fundamental Considerations for Optimal Grain Growth

This paper is not intended to be a treatise on weld metal grain growth but some fundamental considerations on this subject, relevant to weld development, will be presented. The grain size and growth direction are most important in this regard. Grain growth in these welds is essentially entirely epitaxial growth from preexisting grains in the base metal. In this fcc metal, the <100> is the easy-growth direction. Thus, grains with that orientation relative to the temperature gradient direction tend to grow at the expense of other less ideally oriented grains. This accounts for the considerable grain coarsening seen as the solidification front grows away from the FZ boundary. Additionally, the epitaxial growth from the base metal grains tends to occur most strongly in the direction of maximum temperature gradient.

Based on the early weld development on DOP-26, it seems that the most important weld variable relative to grain growth is travel speed. Thus, a discussion of travel speed effects from Liu and David [9] will be paraphrased here. At slow travel speed the weld pool is nearly circular and the temperature gradient is relatively constant in magnitude but changes direction continuously from being normal to the travel direction at the edge of the FZ to being along the travel direction at the weld center-line. In that circumstance where the temperature gradient is continually changing (and with a fine grained base metal) none of the individual grains can grow to a large extent relative to others. In that case, the weld center-line tends to consist of multiple grains that distribute the segregated solute and the cooling stress over a large grain boundary area. At higher travel speed the weld pool becomes a bit more elongated and the temperature gradient changes considerably from the edge to the center of the weld pool. In that case the easy-growth direction oriented grains will dominate the initial grain growth and will continue to outgrow the less preferentially oriented grains all the way to the weld center-line. At this intermediate travel speed the weld center-line will often consist of only a few large grains growing together in a plane through the weld thickness direction. Finally, at even higher travel speeds the grain growth changes qualitatively. In this case the weld transitions to the pronounced teardrop shape. Because of the higher solidification rate the easy-growth directionality becomes less important (the solidification mode becomes more similar to equiaxed dendritic). In this case the grain growth terminates at abutting fronts along the center-line and forces considerable solute segregation at the center-line creating a very crack prone structure. Schematic illustrations of the proposed travel speed effects on grain growth (from David and Liu [9]) are shown in Figure 21. Pictures of welds that illustrate the basic travel speed dependence seen during laser welding of DOP-14 are shown in Figure 22. This illustrates why weld development for DOP-26 largely considered travel speeds in the range of 10 – 25 mm/s.

A very interesting structure arises at intermediate travel speeds. In this case, the overall grain growth results in nearly parallel straight grains growing together at the weld center-line. As the grain growth continues, several small grains tend to nucleate and grow parallel to the weld travel direction (the right hand picture in Figure 22). The result of this is a very prominent center-line consisting of essentially one continuous grain boundary through the weld thickness direction. This structure is probably also deleterious to weld impact properties.

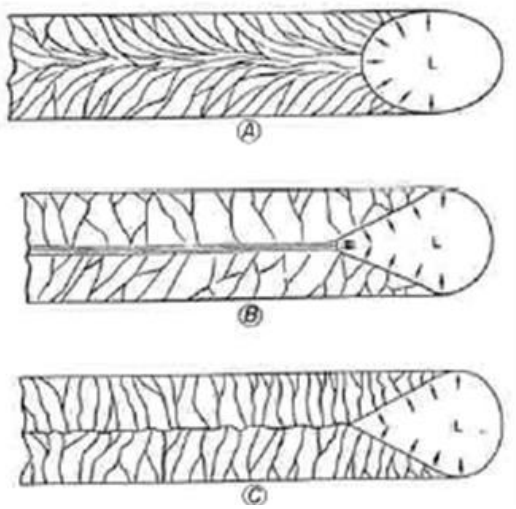

Figure 21: Schematic illustrations of the weld zone grain growth expected for different weld travel speeds (from [9]).

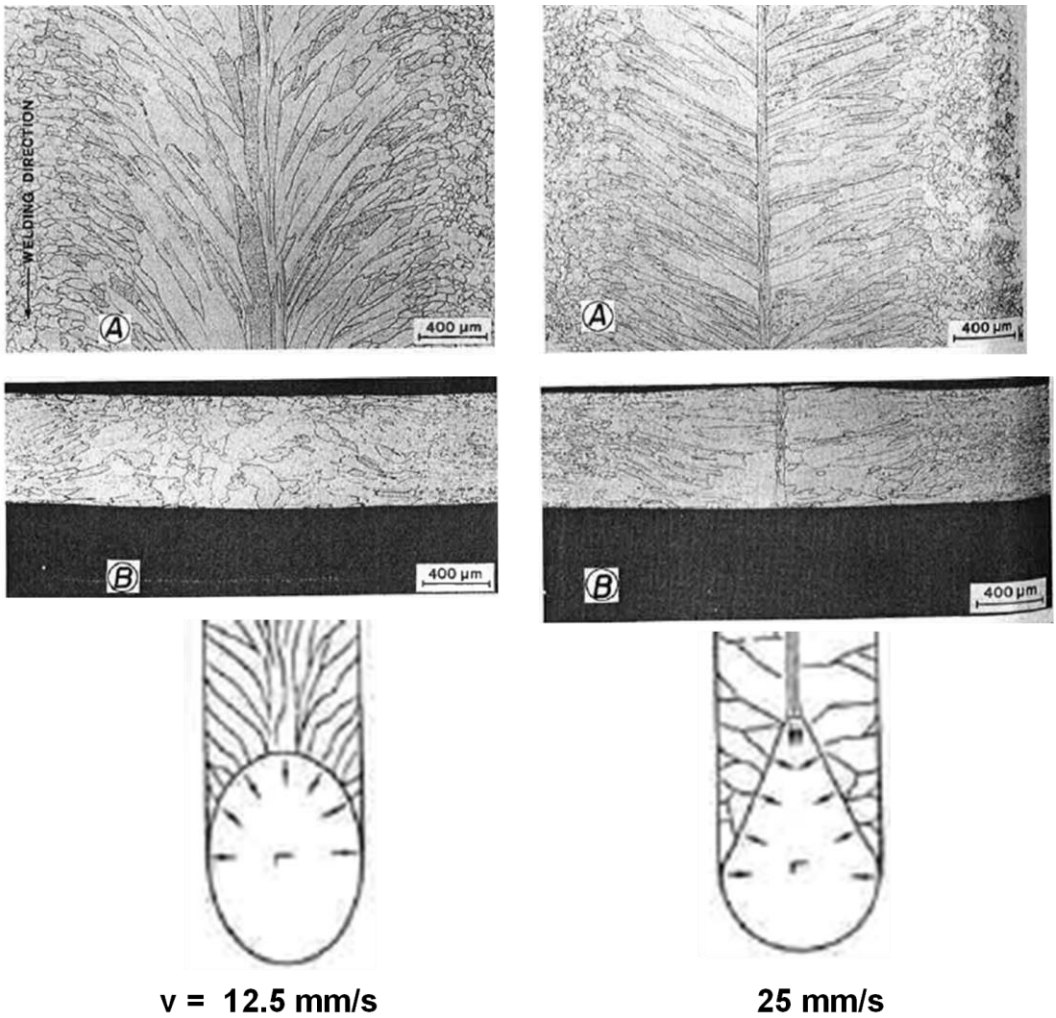

Figure 22: Picture of the weld grain growth behavior for different weld travel speeds observed in laser welds on DOP-14 material (from [9]).

It seems likely that this important center-line structure is a result of thorium segregation and the attendant effect of this on weld metal melting point. The degree of thorium segregation to the weld center-line is at least X 20 that of the bulk of the weld [26] and is consistent with formation of the Ir-Th eutectic in that region of the weld. Dendritic growth in this last-to-solidify material would respond to the temperature gradient in this location, which is essentially entirely parallel to the weld travel direction, and would be largely independent of the epitaxial growth that preceded this structure. The important point is that the existence of this particularly deleterious structure would be sensitive to travel speed but also highly sensitive to the degree of thorium segregation to the weld center-line. This suggests that original alloy composition of thorium as well as the quantity of base metal melted is very important to weld impact properties. Thus, considerable weld metal sensitivity to overall input power and weld width (arc length therefore being important) is expected.

Other possible welding variables could be important to providing an optimal weld metal grain structure. In keeping with early weld development on iridium (as in [15]) the possibility of grain refinement through arc oscillation is a possible process variant. Some data showing possible useful grain refinement with arc oscillation is illustrated in Figure 23. (Actually it should be noted that overall weld width appears to be substantially different in those two welds and it is not entirely clear that substantial grain refinement from the oscillation occurred). Other processing variants such as current pulsing may also produce useful grain refinement.

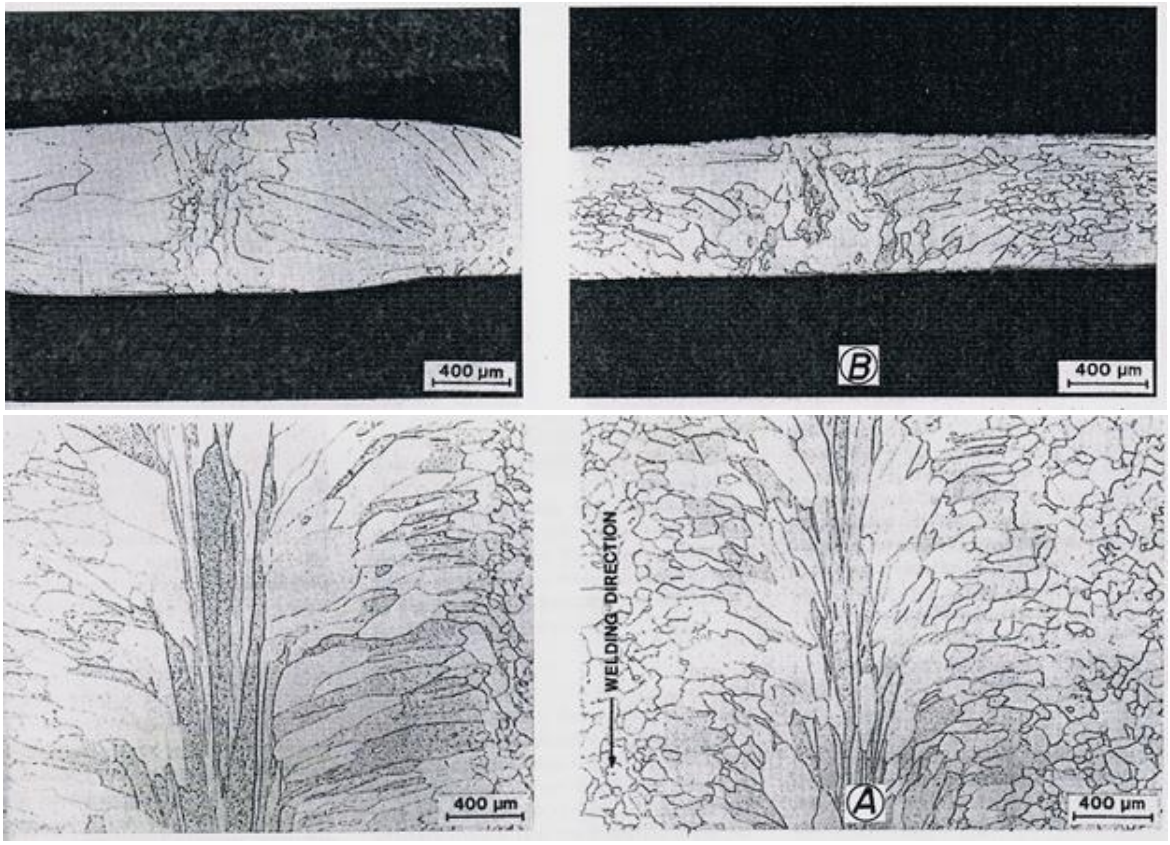

Figure 23: Photos of the top surface and metallographic sections of GTA welds on DOP-26 made with (right hand pictures) and without (left hand pictures) 6.25 Hz arc oscillation, from [9].

The initial useful work on optimizing the DOP-26 welds came from Liu and David [17]. In this work, flat coupons with the nominal GPHS wall thickness were made. These coupons were vacuum annealed to provide a fully recrystallized base metal grain structure. Spark source mass spectroscopy was used to show that the resulting coupons had compositions near to the nominal values for DOP-26. At that point a series of GTA welds were made on those coupons for the purpose of exploring the mechanical properties of those welds. The welds were made with a travel speed of 12.7 mm/s in a 75He-25Ar atmosphere. There was no elaboration on the welding variables used but they were clearly chosen to achieve full penetration and with some variation in cooling rate. Apparently the 6.25 Hz transverse arc oscillation was used.

The basic intent of the experiments of Liu and David [17] was a comparison of properties of welds that were wide (variables adjusted to achieve 3.7 mm top surface beam width) versus narrow welds (variables adjusted to achieve 2.5 mm top surface width). It is not clear how these weld shapes were actually achieved but it seems that this was accomplished largely through positioning of chills around the weld. After welding the specimens were given a post-weld heat treatment at varying temperatures and durations (1500 C for 1 hr was a typical PWHT). Pictures of the resulting welds are shown in Figure 24. Notice that the narrow weld center-line consisted of multiple through-thickness grains while the wide weld shows the pronounced center-line structure that is expected to be particularly deleterious to fracture behavior.

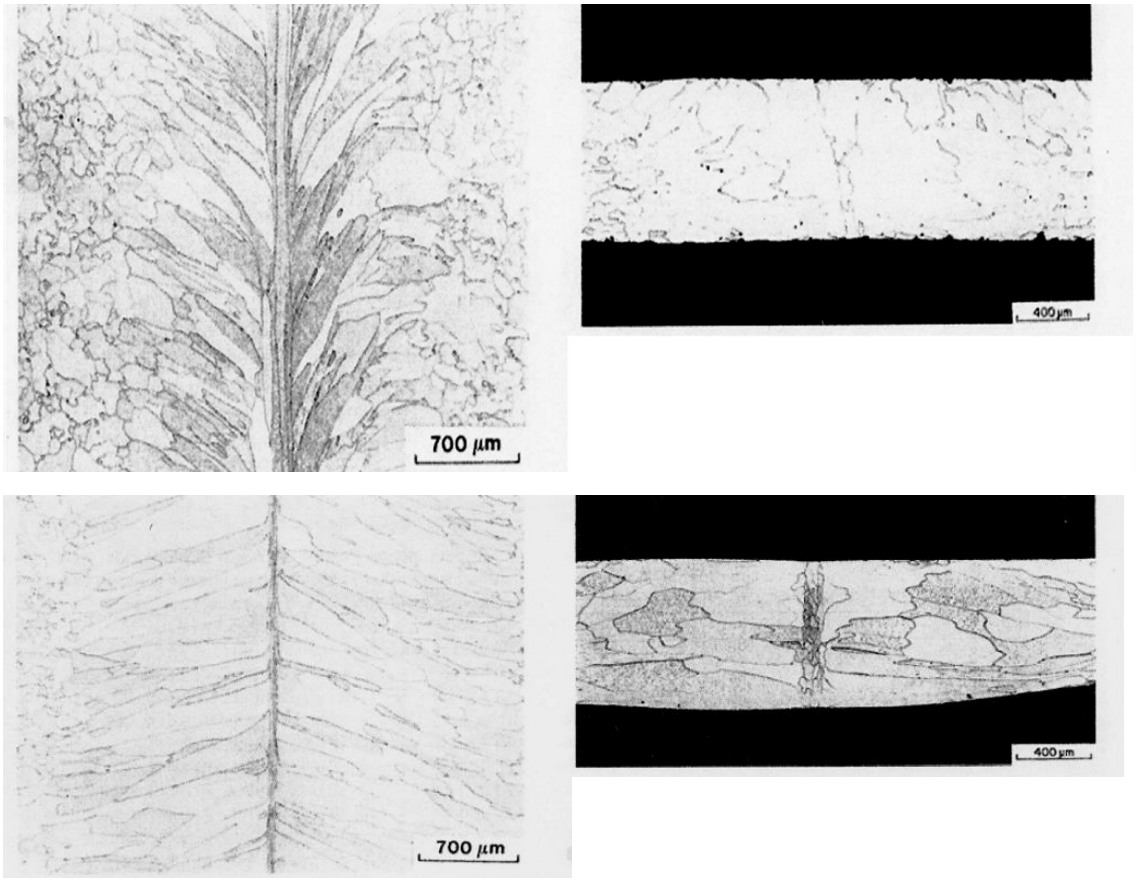

Figure 24: Photos of the top surface and metallographic sections of narrow (A) and wide (B) GTA welds on DOP-26, from [17].

A variety of mechanical tests and metallurgical evaluations of welds on the DOP-26 alloy were made by Liu and David [17] (note that this is “old process” material). They did perform typical mechanical as well as impact testing on specimens that tested the transverse and longitudinal (relative to the weld travel direction) behavior of the weld metal. In this review the transverse behavior will be discussed since that would seem to be most relevant to weld performance relative to part serviceability. For all of the tests, the longitudinal impact behavior was substantially better than the transverse.

The following table (copied from [17]) summarizes the standard mechanical test results of the DOP-26 welds. The first important point made here is that the mechanical behavior of the

Table II. Tensile Properties of DOP-26[a] Gas Tungsten Arc Welds Tested at 650 °C at a Crosshead Speed of 25 mm Per Minute

Bead Width[b]	Weld Type	Postweld Heat Treatment (h)	Postweld Heat Treatment (°C)	Weld-Test Orientation[c]	Elongation (Pct)	Strength (MPa) Yield	Strength (MPa) Tensile
Wide	BOP[d]	None		Transverse	2.0	169.5	211.5
Wide	Butt	None		Transverse	3.1	164.7	291.5
Wide	Butt	1	1500	Transverse	4.3	119.9	275.6
Narrow	Butt	None		Transverse	10.5	173.6	508.5
Narrow	Butt	1	1500	Transverse	14.3	137.8	545.0
Narrow	Butt	1	1500	Longitudinal	21.5	164.7	462.3
Base metal[e]					31.2	85.4	530.5

[a]DOP-26 annealed one hour at 1500 °C before welding.
[b]Wide, 3.7 ±0.2 mm; narrow, 2.5 ±0.2 mm.
[c]Transverse: specimens with a weld perpendicular to the tensile direction. Longitudinal: specimens with a weld parallel to the tensile direction.
[d]Bead-on-plate welds.
[e]Specimens annealed one hour at 1500 °C before testing.

narrow welds is considerably superior to the wide welds. For example, the elongation at failure of the wide and narrow welds are 4.3% and 14.3% respectively. The table also shows the considerable improvement in mechanical properties that resulted from post-weld heat treatment of 1500 C for 1 hr (roughly 30% improvement in properties). The authors attributed this to relaxation of residual stress during the PWHT since essentially no change in grain structure during PWHT was seen. SEM examination of the fracture surfaces (note: this is a relatively low temperature, 650 C, tensile test where iridium does exhibit brittle behavior) revealed that the fracture surfaces all showed brittle behavior. In the base metal the fracture tended to be transgranular with secondary cracking. However, in the weld metal the fracture tended to be primarily intergranular (in the narrow weld, transgranular failure occurred near the weld center-line and became intergranular nearer the FZ boundary).

The most important property of the welds relative to part serviceability is impact ductility. This was tested for the series of welds made by Liu and David [17] and those results are summarized in Figure 25. The most important point in this figure is that the impact elongation, at the now standard test conditions, was considerably different for the wide and narrow welds. The narrow weld showed an impact elongation of about 8% while the wide weld elongation was only about 4%. It is interesting to note that these elongation values are entirely consistent with grain size behavior. Referencing data such as in Figure 8, the base metal results suggest a grain size of about 40 microns while the narrow weld results suggest a grain size of about 120 microns. These values are consistent with the actual observed grain sizes. The wide weld results are also consistent with this but in a bit different way. The analysis suggested by Figure 8 really only applies to relatively small grain size. The low fracture of elongation seen in the wide weld is consistent with the baseline intrinsic grain boundary strength value (ie. is consistent

with a single grain boundary extending through the weld – consistent with the metallography of that weld). The fracture surfaces resulting from the impact test indicated that the fracture was similar to that seen in the lower temperature standard mechanical test. In this case, the authors did note significant particulate (presumably Ir_5Th precipitates) and porosity on the grain boundary facets. In the case of the wide weld some of the fractured grain boundary facets did show patches of material consistent with the Ir + Th eutectic, which would further limit grain boundary strength.

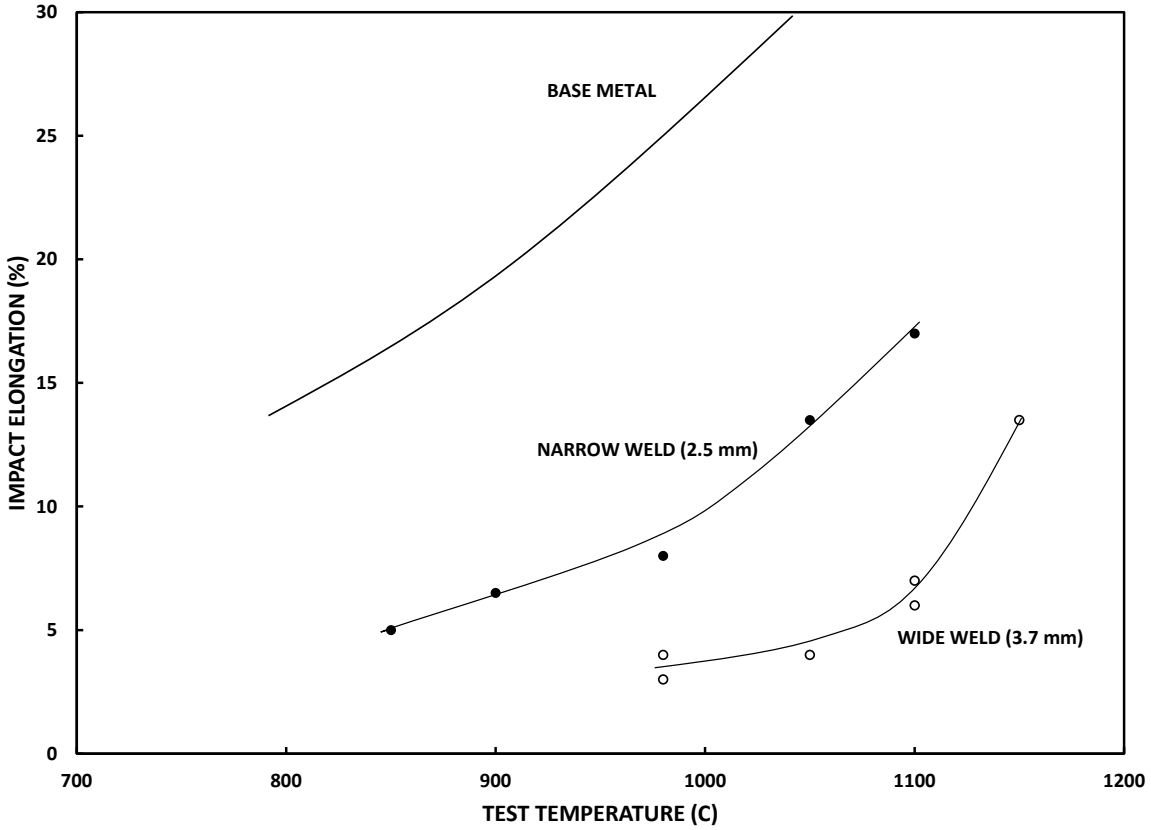

Figure 25: Impact elongation versus test temperature for base metal and weld metal, from [17].

These data from Liu and David [17] are undoubtedly the reason that the GPHS processing specification requires that the maximum weld width be limited to about 3 mm. This is essentially mid-way between the "narrow" and "wide" conditions reported in this work and should be expected to yield an impact elongation of > 5%, which is consistent with the value required for appropriate impact resistance of the GPHS unit. Specifying a maximum weld width is realistic especially in a situation where the potential for weld solidification cracking is lurking as a possibility. However, it should be noted that the real requirement on the weld metal is that it should consist of multiple interlocking grains especially along the thickness direction of the weld. Weld width is clearly important in this regard because higher input power per unit length generally yields larger grain size but the real requirement is the grain morphology. The exact weld variables used to achieve the appropriate microstructure are essentially unimportant as long as the result is appropriate.

The impact test continues to be part of standard material acceptance testing at ORNL. Some of that more recent data was provided to us by: Miller [7] as well as McKamey et. al. [18]. Some useful data from [18] are shown in Figure 26. This represents additional data on impact

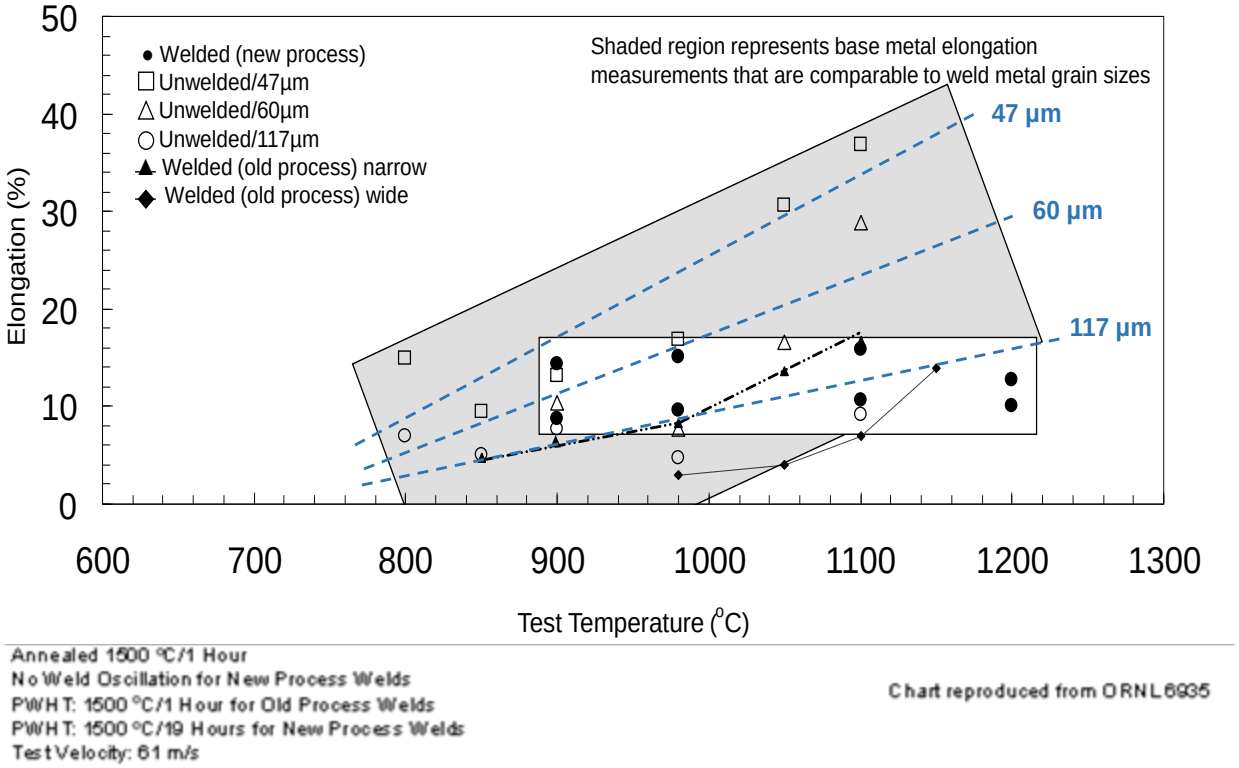

Figure 26: Impact elongation versus test temperature for base metal and weld metal including some comparison of "old" and "new" process DOP-26, from [18].

elongation obtained circa 1998. The new useful information in this figure is a more direct measurement of impact properties versus average grain size of the base metal. The dashed blue lines on Figure 25 are approximate "guides to the eye" that illustrate how the impact elongation of the base metal responds to grain size. Note that the weld data for DOP26-NP were generated using the typical weld variables used in the Sigmajig test (It is important to note that these tests are not performed at the "production" welding parameters. It is also important to note that these data show good weld metal elongation with no arc oscillation being used). Comparing the results for DOP26-OP and DOP26-NP shows that weld metal impact behavior has always been basically consistent with the resulting grain size in the weld metal. The impact data for "wide" GTA welds on DOP26-OP do seem to be a bit anomalously low. However, without more details of how those welds were made any further conclusions are impossible. It is also important to note that impact elongation of GTA welds, tested at the standard 980 °C, does seem to be a bit better for recent welds on DOP26-NP than it was for similar welds on DOP26-OP. This may suggest that material processing continues to improve with time.

PRODUCTION EXPERIENCE AND 4-POLE MAGNETIC ARC OSCILLATION (MAO)

The early welding studies of DOP-26 suggested that a high energy density process would be ideal for this welding. However, for various programmatic reasons it was decided to produce the GPHS using the GTAW process. Therefore, a semi-automatic GTA process was developed for this production at the Savannah River Plant. This work occurred in about 1983. A summary of the initial weld development efforts for this work were presented by Kanne [19]. Based on the historical data, the starting point welding variables for this process development were: travel speed = 12.7 mm/s (8 rpm); He+25%Ar shielding gas; arc current = 83 A; transverse magnetic arc oscillation at 6.5 Hz to help promote the desired grain structure. No details of the MAO were given but it appears from the top surface picture (Figure 27), that the oscillation amplitude was about +/- 0.25 mm.

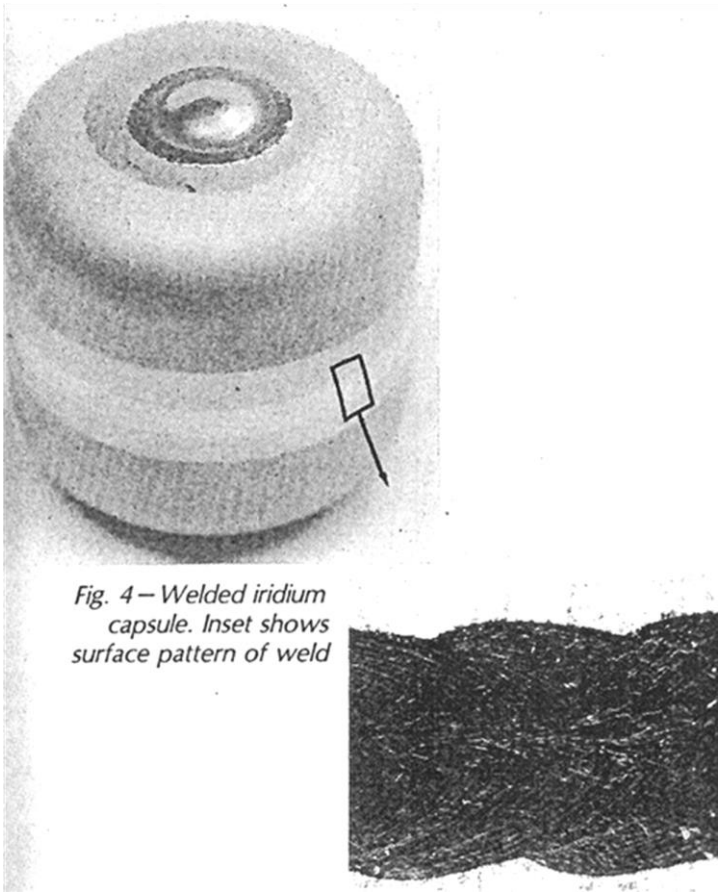

Figure 27: Picture of welded GPHS and weld top surface close-up, from [19].

Kanne [19] also described some details of the weld development welds showing that the desirable grain structure can be produced in various ways. Figures 28 and 29 illustrate that the desired relatively equiaxed grain structure will be produced by the appropriate combination of travel speed and power input. In general, the welds were kept as narrow as possible and the power versus travel speed (with travel speed generally held at 12.7 mm/s) were adjusted to yield good microstructure with full joint penetration around the GPHS clad.

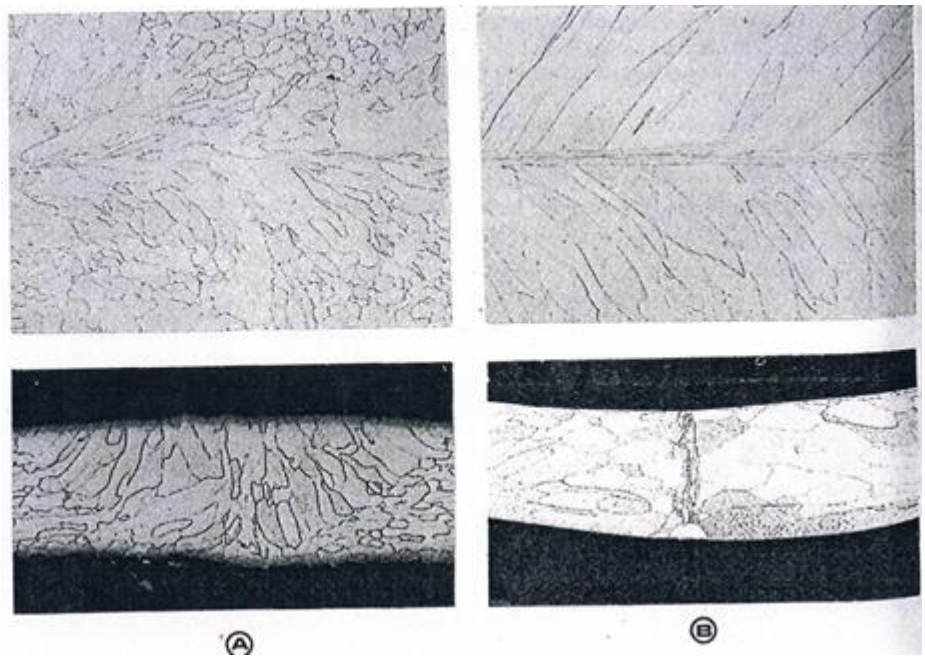

Figure 28: Effect of arc power on weld microstructure resulting at 12.7 mm/s for: A – minimal arc current (2 mm wide); B – somewhat excessive arc current (3 mm wide), from [19].

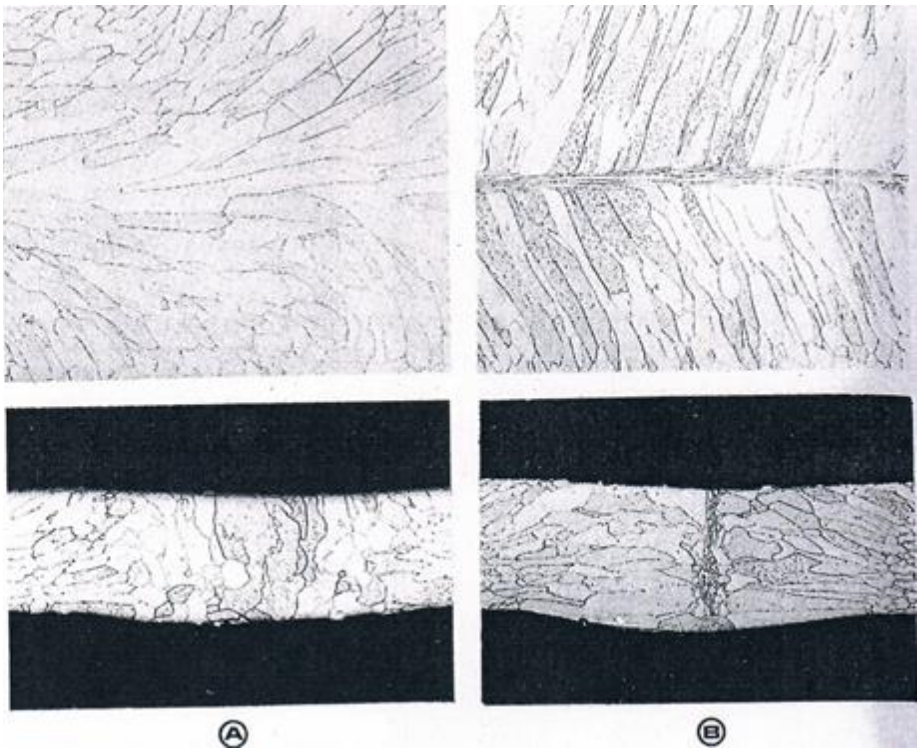

Figure 29: Effect of welding speed on weld microstructure for nominal arc current and for: A – 4.6 mm/s; B – 15.7 mm/s, from [19].

The weld development activities on DOP26-OP were generally successful but a high percentage of the welds showed cracking at the weld quench, where the arc current is sloped towards zero after one full revolution plus a bit of weld overlap. Figure 30 shows a picture of the inside surface of a welded clad showing these cracks. Figure 31 is a schematic drawing showing the location of the cracks. The cracks were typically about 5 mm long with the most prominent cracks being along the weld center-line.

Figure 30: Picture of the inside surface of a typical weld showing the “weld quench” cracks.

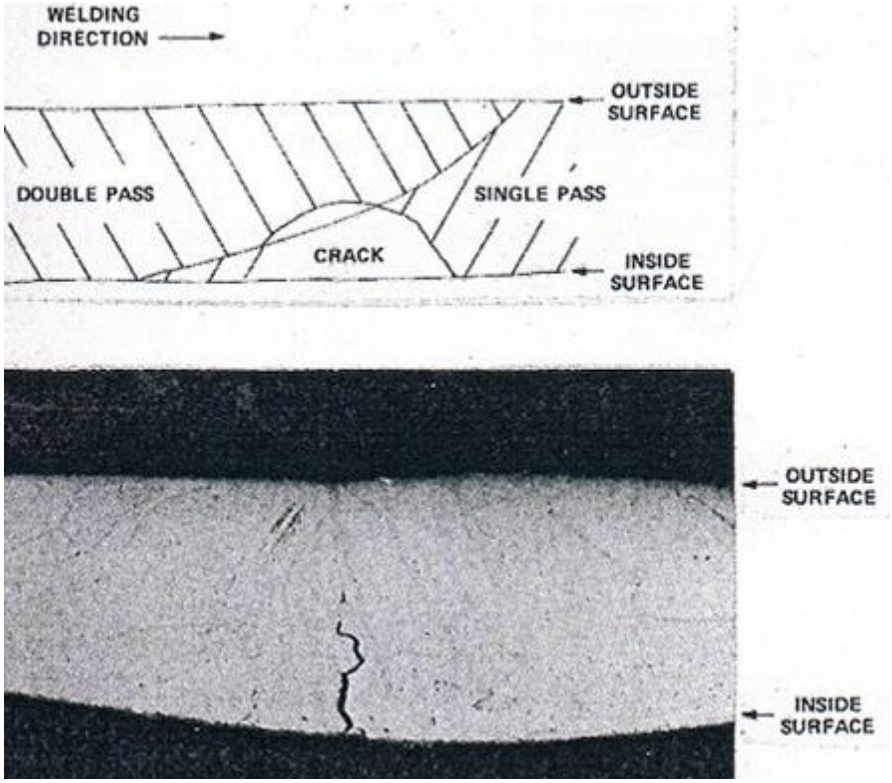

Figure 31: Schematic of the weld showing the location of the crack relative to the arc slope-out and a weld cross-section showing a weld center-line crack, from [19].

Kanne [19] attributed this cracking behavior to a combination of grain liquation in the existing weld metal immediately ahead of the remelt fusion zone and the complex stress state of weld metal in the weld quench area. Some corroborating evidence for the likelihood of grain boundary liquation was obtained with SEM imaging of the fracture surfaces. Figure 32 shows a

Figure 32: SEM picture of a crack face in the weld quench area in the DOP26-OP material showing the ridge structure indicative of eutectic formation on that grain facet, from [19].

typical weld fracture surface showing the ridge networks on a grain facet indicative of eutectic melting that covered essentially all of that grain facet. Additionally, scanning auger microprobe analysis of crack faces showed thorium concentrations there to be up to 30 at-%. This is consistent with formation of the Ir + Th eutectic, which melts at 2080 C.

The exact location of the majority of these cracks, namely in the weld overlap area but ahead of the actual remelt zone, is interesting. There are probably two factors involved in this observation. First, the initial weld metal has had a limited time to cool (roughly 8 seconds) and will still be fairly hot. As the second weld pass approaches, the 2080 C eutectic meting point will be exceeded substantially ahead of that fusion zone. (Note: a simple 2-D heat flow model of this weld shows that eutectic melting of grain boundaries would occur about 0.4 mm ahead of the FZ of the second pass weld.) Second, the cooling stress on the existing weld metal will change its magnitude and directionality as the second weld pass approaches.

Some progress towards eliminating these cracks was made by minimizing power input and minimizing arc length. Additionally, a bit longer arc current slope-out was somewhat helpful. Nevertheless, roughly 20% of welded units showed the cracking behavior with the crack size having been minimized to be perhaps 2 mm long and 0.1 mm deep. It is interesting to note that

the propensity for cracking did seem to depend considerably on the batch of DOP-26 being used. Some batches of DOP26-OP yielded zero cracking while other batches yielded 25% cracked welds. As we have seen, this is probably a result of considerable variability in thorium content that was common in DOP26-OP base metal.

Assuming that the cracking behavior is actually center-line cracks primarily caused by the considerable thorium segregation to that area, improvements in that cracking would result from further adjustment of grain growth (ie. a more refined grain size would help and additionally, any process modifications minimizing thorium segregation would also improve cracking susceptibility). In keeping with all of the previous weld development activities, improvements in arc oscillation was the primary process variable investigated further.

Up to this point in process development, arc oscillation had been used but it was a simple setup that only resulted in transverse arc oscillation. Therefore, a more sophisticated magnetic arc oscillator (MAO) was procured and installed on the production equipment. This MAO produced both longitudinal and transverse arc oscillation with the amplitude of the two axes of oscillation being independently controllable. This has come to be known as “four-pole oscillation”.

The basic oscillation parameters eventually used for production consisted of: an elliptical oscillation pattern at 50 Hz and with the lateral oscillation amplitude set to that previously used (reportedly 0.13 mm) and longitudinal amplitude about double that (therefore, about 0.26 mm). Production success of this process modification was reported by Scarbrough and Burgan [20]. Production success (units without detectable internal cracks) with the new MAO was quite good. The overall failure rate due to cracked welds was 2% at this point (contrast to the failure rate of roughly 20% with 2-pole MAO). It is interesting to note that the batch-to-batch variation in material crack susceptibility (ranging from batches with 0% to some with up to 26% failure without MAO) was mostly eliminated; all batches when using the 4-pole MAO showed a comparable 2% failure rate. This means that the new MAO was highly effective in mostly eliminating the arc quench cracking failures. At this point some discussion of the possible fundamental mechanisms related to MAO success is important for assessing the future value of MAO relative to other possible welding procedures.

The first possible way that MAO helps cracking susceptibility has been apparent throughout weld development. MAO does produce some amount of grain refinement. Scarbrough and Burgan [20] report a 17% reduction in average grain size when using 4-pole MAO versus the original 2-pole MAO (actually, their data shows about a 12% grain size reduction at the weld center-line, which would seem most significant to this problem). Smaller grain size may be useful in this case because this would yield a greater grain boundary area over which the segregated thorium is distributed and perhaps keep the eutectic patches seen on grain faces small enough that cracking cannot initiate. Of course, smaller grain size generally yields a better fracture toughness to the weld in general.

Additional studies reported by Scarbrough and Burgan [20] present two other interesting possibilities for the MAO improvement. The first interesting observation was “pulsation” of the weld pool seen on high speed photographs of the weld during MAO. The mechanism for this isn’t obvious but could be surface depression induced by arc force pressure or perhaps changes

in surface tension (and hence, surface shape) with surface temperature. In either case, it is possible that MAO is driving fluid motion in the weld pool, which would distribute the thorium away from the weld center-line and perhaps minimize segregation of thorium to grain boundaries at the critical weld center-line. An additional interesting observation is that the longitudinal MAO is of a sufficient magnitude that the arc "decouples" from the weld pool at the extremes of the oscillations. In this context, "decoupling" apparently refers to initiation of local freezing in the weld pool as the arc moves to the extremes of its oscillation. Scarbrough and Burgan [20] refer to this periodic freezing as creating a "damming" effect blocking the movement of thorium along with the solidification front. Variable cooling rate would affect dendrite growth as well as the thorium distribution at the solid liquid interface (a diffusion process). Thus, variable cooling rate could act to deposit thorium in the interdendritic spaces and thus in the grain substructure. This could decrease thorium segregation to the weld center-line and minimize the weld quench cracking likelihood. An additional possible effect of longitudinal MAO is that this makes the arc input power somewhat elongated in the weld travel direction. In effect, this would produce some amount of weld pre- and post-heat and would act to somewhat decrease stress localization around the weld.

A detail of the quoted MAO parameters is worth some discussion. In this review we can only trust that the quoted oscillation amplitude values of 0.13 X 0.26 mm are correct. However, it is a bit questionable that a movement of the arc by that small amount (note that the weld pool is roughly 4 mm long in this weld) cycling at 50 times per second could produce a noticeable periodic freezing/melting at the solidification front. This basic question also arises in connection with how the arc oscillation was measured. Such a small arc deflection on an arc of nominal arc length equal to 0.9 mm would be difficult to measure accurately by any usual technique, such as high speed video. It remains possible that the quoted oscillation values are simply erroneous. Additionally, quantitative characterization of the MAO by data acquisition was never done in production. It is not known how repeatable MAO was in actual GPHS production. In any case, accurately measuring, controlling and calibrating this small arc oscillation is obviously difficult. This fact is clearly important to the possible incorporation of MAO into future production welding of the GPHS.

A final important consideration relative to this cracking issue is that this weld development and fabrication work was done with DOP26-OP material. There are three important possible problems with this material. First, it is known that it did contain some level of non-metallic impurities that segregated to grain boundaries. That would make the cracking problem worse. Second, the melting practice at that time often left the material improperly homogenized relative to the thorium distribution. Third, the actual thorium content of the material could vary by at least +/- 50% (note: this was largely a result of the chemical analysis methodology, which had not been properly optimized at that time). The result of the latter two problems is that some batches of DOP26-OP (and/or isolated areas in any particular batch) could easily have had thorium contents up into the 100 wt-ppm range where weld cracking is essentially inevitable. This means that welding results on the DOP26-OP material may not be representative of results to be expected on DOP26-NP.

Additional Weld Development and Fabrication after 1988: DOP26-NP

Starting in about 1988 process requalification efforts began in preparation for another GPHS fabrication run at SRP. Since considerable material processing changes had occurred prior to this, some fundamental studies of DOP26-NP material were undertaken. The essential assumption in this work was that the previously used production parameters would undoubtedly be used and the basic purpose of this work was to demonstrate process viability for the new material.

In this regard, Kanne [21] devised a weld test to look specifically at the weld overlap cracks seen in previous production. A bit different test is required because the usual weld coupon studies (including Sigmajig) do not address the issue of weld overlap. The test devised by Kanne was to use full capsule assemblies. These were then fully welded with the usual production weld schedule. Following that several short segment welds were made over the welded area (basically equivalent to crater cracking studies). Cracking in the weld overlap and in the short weld segments were then counted. Capsules made of DOP26-OP were compared with those made from DOP26-NP. Because of the fairly limited number of welds made, the statistical significance of the results is a bit questionable. However, the total number of cracks seen in DOP26-NP was about 45% of the number seen in DOP26-OP. This included a fairly high percentage of total cracks being basically crater cracks in the short segment welds (crater cracking is a rather conservative way to estimate material cracking susceptibility because of the highly concentrated stress generated in that situation). Most importantly, the number of weld overlap cracks seen in DOP26-NP was about 20% of the number seen in DOP26-OP. This work demonstrated that the likelihood of weld overlap cracking was considerably minimized by the “new process” melting practice.

Sigmajig testing was also performed on the DOP26-NP material and reported by: by Ohriner and Goodwin [22]. The Sigmajig tests were performed with the usual welding parameters for this test (different from production parameters): 125 A; 12.7 mm/s travel speed; 0.9 mm arc length; pure argon shielding. Tests were performed with and without MAO. These tests showed that the details of MAO shape (elliptical versus longitudinal) were relatively unimportant so mostly longitudinal MAO was used. Presumably, the oscillation amplitude was set to the usual production value (reported as being 0.13 mm transverse, where used, and 0.26 mm longitudinal). The results of the Sigmajig testing are summarized in Figure 33. As can be seen, MAO did increase the threshold cracking stress by about 20% relative to welds with no arc oscillation. Further, it appears that the optimal oscillation frequency is about 10 Hz. It is interesting to note that the Sigmajig threshold cracking stress is little improved by MAO for high oscillation frequency (ie. $f > 20$ Hz). Thus, there is no ready explanation for why the production oscillation frequency of 50 Hz was used since it would provide little net improvement in cracking susceptibility in the DOP26-NP material.

The most significant result from this work is that the threshold cracking stress for DOP26-NP was nearly double that for DOP26-OP. Obviously, the need for an optimized MAO process was greatly reduced in the “new process” material.

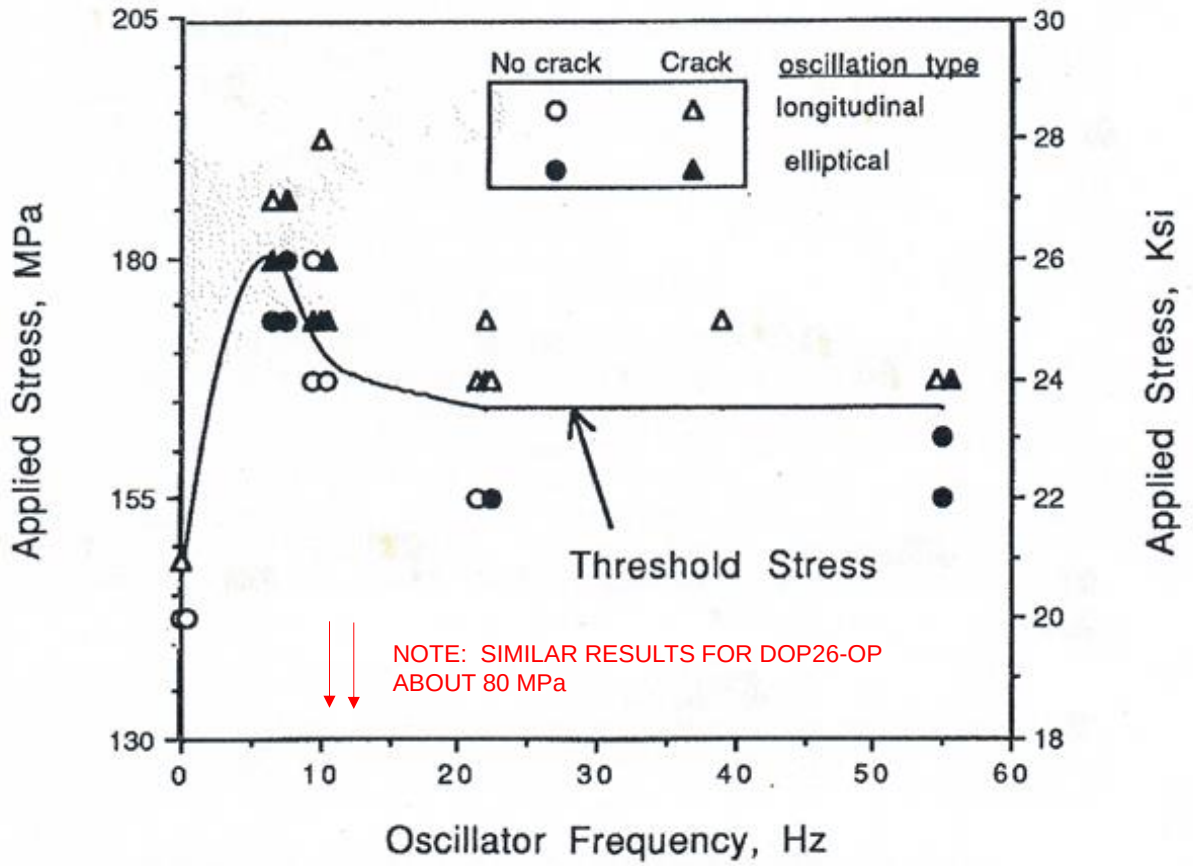

Figure 33: Sigmajig threshold cracking stress versus MAO frequency for DOP26-NP, from [22].

Another critical result presented by Ohriner and Goodwin [22] is related to grain structure in the DOP26-NP material. Figure 34 shows metallography of typical DOP26-NP welds made with and without MAO. As can be seen, there is no apparent grain structure modification provided by MAO in this material. The critical point is that the benefits of MAO on the "new process" material are greatly diminished. It remains to be proven that MAO is still necessary to provide good weld quality and whether judicious choices of other welding variables such as arc power, travel speed and current pulsing might produce similarly good results.

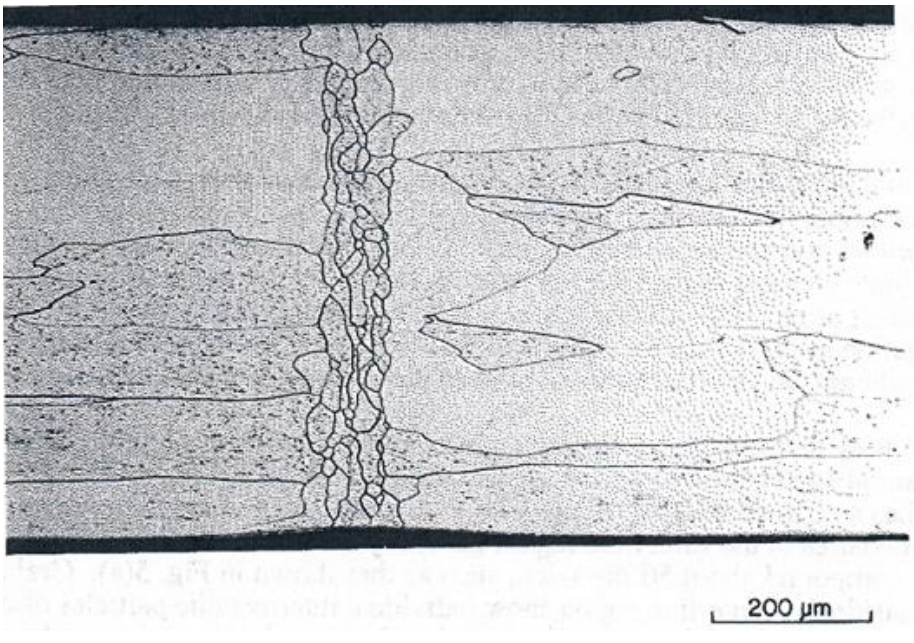

(A)

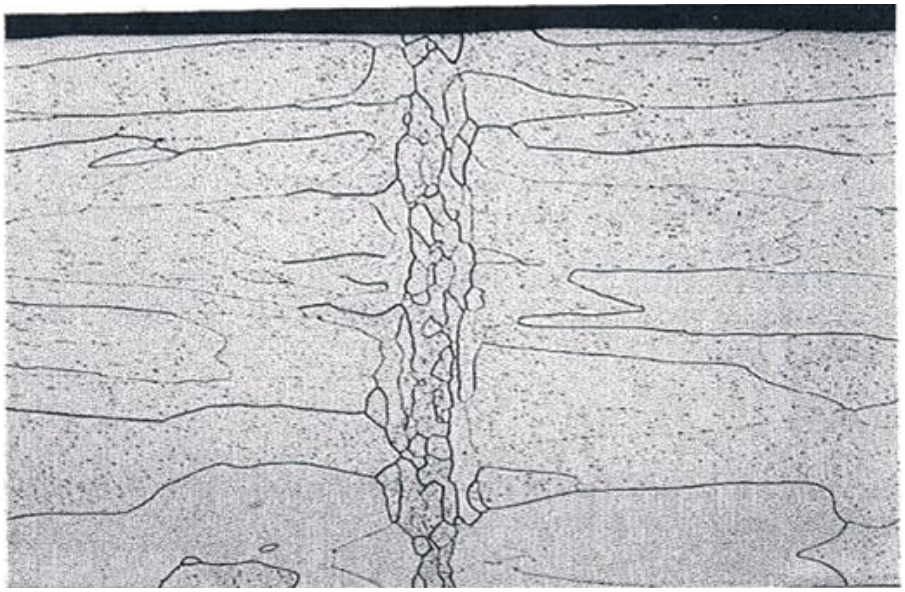

(B)

Figure 34: Metallography of welds made on DOP26-NP without, (A), and with, (B), the 55 Hz magnetic arc oscillation, from [22].

The results from the ensuing production welding using DOP26-NP were summarized by: Franco-Ferreira and George [23]. The basic welding parameters used are summarized in the following table.

Parameter	Material/Setting/Value
Tooling-ring composition	Type 304 stainless steel
Tooling-ring screw torque	20 in.-lb
Capsule end load	30 lb
Welding current	55 A for 0.5 s 115 A rising to 116 A in 7.3 s 116 A tapering to 22 A in 3 s
Arc voltage	Initial arc length set at 0.035 in. Measured average value: 15.6 V
Travel speed	0 for 0.5 s 29.5 in./min for 10.3 s
Weld start offset	8 deg from vent slot
Magnetic arc oscillation	
Frequency	55 Hz
Cross-seam amplitude setting	11%
Longitudinal amplitude setting	100%
Torch gas	30 ft^3/h 75% He/25% Ar

The production run met with good success. A relatively small number of the production units (roughly 3.5%) were rejected due to some misalignment of the ID surfaces of the two cup ends (the unit had a butt joint brought into proper alignment and then tack welded; some joint offset using procedure is inevitable). Most importantly by the end of this production run, 450 units had been made with 0% failures due to weld cracking.

Two important things were noted in connection with this production run by: Franco-Ferreira and George [23]. The first problem noted was variable weld penetration around the part. At the nominal wall thickness, adequate weld penetration was achieved with an arc current of about 105 A. However, this resulted in areas of lack-of-penetration in the actual assemblies. Thus, a nominal weld current of 115 A was eventually adopted, which yield an over-penetrated weld in places around the part (thereby consuming the internal weld shield). This weld penetration variation was traced to a noticeable, about 8%, variation in cup wall thickness around the part. This happens because the forming blanks for the cups start as rolled plate. The rolling induced residual strain does produce some difference in wall thickness as the cups are drawn.

It is important to note that over-penetration and melting of the weld shield is undesirable for several reasons. The first issue is that the weld shield is in the assembly to prevent PuO_2 contamination from entering the weld. Consumption of the weld shield by the weld is contrary to the basic design intent. The second problem with weld shield melting is that this creates a sharply defined crack-like feature at the part ID surface. Part of the acceptance criteria for the weld assemblies is UT inspection to look for defects in the weld. The aforementioned weld shield melting produces a UT indication indistinguishable from a weld crack. Therefore, the part must undergo additional RT testing to determine if a weld crack has actually occurred. This step adds time and cost to the program. A final problem with weld shield melting is that the "notch" created at the shield to cup weld interface can create a stress riser leading to actual weld root cracks.

As a matter of standard practice, the part rolling direction (and hence, the wall thinning) is oriented in a particular way relative to the arc start on the parts to be welded. It seems feasible that modern GTAW control systems could be programmed with varying arc current synchronized to part rotation in order to produce more constant weld penetration.

A second important process variable change noted by Franco-Ferreira and George [23] is related to the tooling rings. Stainless steel tooling ring are attached to each cup prior to welding and are used to properly locate the parts in the weld fixture. In previous production the bottom cup was positioned with a beryllium-copper collet and the upper cup simply fit into a conical cavity in the upper chuck and was positioned by fixture end-load. At that time, the required weld current was 83 A. This arrangement provided imprecise part joint alignment and some out-of-round condition of the upper cup was a problem. Thus, in the Cassini program both the upper and lower cups were clamped into stainless steel tooling rings which then fit into appropriate cavities in the weld fixture. The use of two tooling rings assured proper joint alignment and did help correct part out-of-round conditions. The interesting part if this is that the weld current had to be increased into the 105 A range in order to accommodate the additional chill effect of the tooling rings (this is a roughly 30% increase in arc power – meaning that this chill effect is quite substantial). Since DOP-26 material properties are known to have a considerable dependence on weld metal cooling rate (and specifically on the resulting weld metal grain structure), the influence of heat sinking on weld properties should undoubtedly be given more attention. Of course this also means that initial weld development work usually performed on flat weld coupons and probably with quite different heat sinking, is probably not representative of results on actual GPHS units.

CONCLUSIONS

The literature pertinent to arc welding of DOP-26 iridium alloy was reviewed. The primary conclusion is that the GPHS assemblies will meet the basic design requirements (namely impact ductility) as long as the weld metal grain structure is optimized. Further, the material will have acceptable resistance to weld solidification cracking as long as the weld metal has an appropriate microstructure. This generally means optimization of travel speed versus input power. Additionally (and perhaps most importantly), weld cracking is minimal as long as the DOP-26 thorium content is near to the nominal 60 wt-ppm. Cracking susceptibility becomes large when the thorium content becomes greater than about 100 wt-ppm. Material fabrication must continue to strive for optimal control of the DOP-26 thorium content.

In the past, magnetic arc oscillation (especially longitudinal oscillation) was found to further improve DOP-26 weldability. Material processing changes incorporated after about 1988 considerably improved all aspects of DOP-26 performance. Weldability and high strain rate ductility data on this newer material strongly suggest that the improvements produced by MAO in the past may no longer be essential to weld success. Redevelopment of the process using more modern welding equipment is certainly warranted. The possible replacement of MAO by proper optimization of the other welding variables should be explored.

REFERENCES

1. T.G. George and M.F. Stevens, “High Temperature Impact Properties of DOP26 Iridium”, LAUR-88-843 (1988).

2. C.T. Liu, H. Inouye and A.C. Schaffhouser, ORNL Report, ORNL-5616 (1980).

3. R.L. Heestand, E.K. Ohriner, T.K. Roche, “Advances in Iridium Alloy Processing”, ORNL Report: ORNL/TM-10852 (1988).

4. W. Clanton Mosley, “Grain-boundary Cavitation and Weld-underbead Cracking in DOP-27 Iridium Alloy”, Savannah River Laboratory Report DP-MS-82-103, (1983).

5. C.T. Liu and H. Inouye, “Development and Characterization of an Improved Ir-0.3% W Alloy for Space Radioisotopic Heat Sources”, ORNL Report, ORNL-5290 (1978).

6. C.G. McKamey, E.P. George, E.H. Lee, E.K. Ohriner, L. Heatherly and J.W. Cohron, “Impurity Effects on High Temperature Tensile Ductility of Iridium Alloys at High Strain Rate, Scripta Mater. 42, pp. 9-15 (1999).

7. R.G. Miller, ORNL, Personal Communication (2016).

8. L. Heatherly and E.P. George, “Grain-boundary Segregation of Impurities in Iridium and Effects on Mechanical Properties”, Acta Mat., 49, pp. 289-298 (2001).

9. S.A. David and C.T. Liu, “High-power Laser and Arc Welding of Thorium-doped Iridium Alloys”, Welding Journal., 61 (5), pp. 157s – 164s (1982).

10. G.M. Goodwin, “Development of a new hot-cracking test – The Sigmajig”, Welding Journal 68(1), pp. 33s-38s (1987).

11. S.A. David, E.K. Ohriner and J.P. King, “Welding and Weldability of Thorium-doped Iridium Alloys”, Iridium, The Minerals, Metals and Materials Society, pp. 325-331 (2000).

12. G.M. Goodwin and E.K. Ohriner, “Sigmajig Weldability Testing of New and Old-Process DOP-26 Iridium Alloy”, ORNL Letter, #0430-34-93 (1993).

13. E.K. Ohriner, G.M. Goodwin and D.A. Frederick, “Weldability of DOP-26 Iridium Alloy: Effects of Welding Gas and Alloy Composition”, CONF. 920104, Amer. Inst. Of Physics Proc., pp. 164 – 170 (1992).

14. S.A. David and J.J. Woodhouse, “Weldability Test for Thin Sheet Materials”, Welding Journal, 66 (5), pp. 129s – 134s (1987).

15. D.L. Coffey, W.H. Jones, W.B. Cartmill and W.A. Saul, “Parametric Modification of Weld Microstructure in Iridium”, Welding Journal, 53(12), pp. 566s – 568s (1974).

16. S.A. David and C.T. Liu, “Weldability and Hot-cracking in Thorium-doped Iridium Alloys”, Metals Tech., pp. 102 – 106 (1980).

17. C.T. Liu and S.A. David, “Weld Metal Grain Structure and Mechanical Properties of a Thorium-doped Ir-0.3 W Alloy (DOP-26)”, Met. Trans. A, 13A(6), pp. 1044 – 1053 (1982).

18. C.G. McKamey, A.N. Gubbi, Y. Lin, J.W. Cohron, E.H. Lee and E.P. George, “Grain Growth Behavior and High-Temperature High-Strain-Rate Tensile Ductility of Iridium Alloy DOP-26”, ORNL Report, ORNL-6935 (1998).

19. W.R. Kanne, Jr., “Welding Iridium Heat Source Capsules for Space Missions”, Welding Journal, 62 (8), pp. 17 – 22 (1983).

20. J.D. Scarbrough and C.E. Burgan, “Reducing Hot-Short Cracking in Iridium GTA Welds Using Four-Pole Oscillation”, Welding Journal, 63 (6), pp. 54 – 56 (1984). As well as SRP report DP-MS-83-83, same authors, same title.

21. W.R. Kanne, Jr., “Weldability of GPHS Iridium Capsules”, Space Nuclear Power Systems, ed. By: El-Genk and Hoover, publ. by Orbit Book Co., Chapter 42, pp. 331 -339 (1988).

22. E.K. Ohriner and G.M. Goodwin, “Letter Report on Effect of Arc Oscillation on the Weldability of DOP-26 Iridium Alloy”, ORNL Report (1991).

23. E.A. Franco-Ferreira and T.G. George, “Cassini Mission to Saturn Relies on Flaw-Free GTA Welds”, Welding Journal, 75(4), pp. 69 – 75 (1996).